

## RECTANGULAR DIAGRAMS OF SURFACES: REPRESENTABILITY

IVAN DYNNIKOV AND MAXIM PRASOLOV

**ABSTRACT.** We introduce a simple combinatorial way, which we call a rectangular diagram of a surface, to represent a surface in the three-sphere. It has a particularly nice relation to the standard contact structure on  $\mathbb{S}^3$  and to rectangular diagrams of links. By using rectangular diagrams of surfaces we are going, in particular, to develop a method to distinguish Legendrian knots. This requires a lot of technical work of which the present paper addresses only the first basic question: which isotopy classes of surfaces can be represented by a rectangular diagram. Vaguely speaking the answer is this: there is no restriction on the isotopy class of the surface, but there is a restriction on the rectangular diagram of the boundary link that can arise from the presentation of the surface. The result extends to Giroux's convex surfaces for which this restriction on the boundary has a natural meaning. In a subsequent paper we are going to consider transformations of rectangular diagrams of surfaces and to study their properties. By using the formalism of rectangular diagrams of surfaces we also produce here an annulus in  $\mathbb{S}^3$  that we expect to be a counterexample to the following conjecture: if two Legendrian knots cobound an annulus and have zero Thurston–Bennequin numbers relative to this annulus, then they are Legendrian isotopic.

## CONTENTS

1. Introduction	2
Acknowledgement	3
2. Rectangular diagrams of a surface	3
2.1. Definitions	3
2.2. Cusps and pizza slices	5
2.3. 3D realizations of rectangular diagrams	6
2.4. Orientations	10
2.5. Framings	11
2.6. Thurston–Bennequin numbers	13
2.7. Which isotopy classes of surfaces can be presented by rectangular diagrams?	14
3. Legendrian links and Legendrian graphs	22
3.1. Definitions. Equivalence of Legendrian graphs	22
3.2. Rectangular diagrams of graphs	24
4. Giroux's convex surfaces	25
4.1. Definition	25
4.2. 'Rectangular' surfaces are convex	26
4.3. Characteristic foliation	27
4.4. The Giroux graph and dividing curves	32
4.5. Proof of part (ii) of Theorem 2	32
4.6. Annuli with Legendrian boundary	37
References	39

---

The work is supported by the Russian Science Foundation under grant 14-50-00005 and performed in Steklov Mathematical Institute of Russian Academy of Sciences.

## 1. INTRODUCTION

Rectangular diagrams of links, also known as arc-presentations and grid diagrams, have proved to be useful tool in knot theory. It is shown in [5] that any rectangular diagram of the unknot admits a monotonic simplification to a square by elementary moves. This was used by M. Lackenby to prove a polynomial bound on the number of Reidemeister moves needed to untangle a planar diagram of the unknot [22].

It is tempting to extend the monotonic simplification approach to general knots and links, but certainly it cannot be done straightforwardly. Typically a non-trivial link type admits more than one rectangular diagram that cannot be simplified further by elementary moves without using stabilizations. As shown in [6] classifying such diagrams is closely related to classifying Legendrian links not admitting a destabilization.

In particular, the main result of [6] implies that the finiteness of non-destabilizable Legendrian types in each topological link type (which is the matter of Question 61 in [4]) is equivalent to the finiteness of the number of rectangular diagrams that represent each given link type and cannot be monotonically simplified. Neither of these has been established so far.

Surfaces embedded in  $\mathbb{S}^3$ , either closed or bounded by a link, have always been one of the key instruments of the knot theory. For studying contact structures and Legendrian links it is useful to consider surfaces that are in special position with respect to the contact structure, so called convex surfaces. They were introduced by E. Giroux in [13] and studied also in [3, 10, 18, 21, 24].

Sometimes one can prove the existence of a convex surface having certain combinatorial and algebraic properties for one contact structure and non-existence of such a surface for the other, thus showing there is no contactomorphism between the structures. This method can be viewed as a generalization of the classical work of Bennequin [1] where he distinguishes a contact structure in  $\mathbb{R}^3$  from the standard one by showing that an overtwisted disc exists for the former and does not exist for the latter. Indeed, an overtwisted disc can be viewed as a disc with Legendrian boundary and a closed dividing curve.

This method can also be used to distinguish Legendrian links by applying the argument to the link complement. For instance, some Legendrian types of iterated torus knots are distinguished in [11] by showing that certain slopes on an incompressible torus in the knot complement are realized by dividing curves for one knot and not realized for the other.

Note that whereas the problem of algorithmic comparing topological types of two links has been solved (see [26]) no algorithm is known to compare Legendrian types of two Legendrian links having the same topological type. Examples of pairs of Legendrian knots for which the equivalence remains an open question start from six (!) crossings [2].

In this paper we propose a simple combinatorial way to represent compact surfaces in  $\mathbb{S}^3$  so that the boundary is represented in the rectangular way. The basic idea of this presentation is not quite new and is implicitly present in the literature. In particular, it can be considered as an instance of Kneser–Haken’s normal surfaces for triangulations of  $\mathbb{S}^3 \cong \mathbb{S}^1 * \mathbb{S}^1$  obtained by the join construction from triangulations of two circles  $\mathbb{S}^1$ .

We observe in this paper that the discussed combinatorial approach appears to be well adapted to Giroux’s convex surfaces with Legendrian boundary. In particular, we show that any convex surface with Legendrian boundary is equivalent (in a certain natural sense) to a one that can be presented in the proposed way.

By using this approach we are going to distinguish some pairs of Legendrian knots that are not distinguishable by known methods. Since a rectangular diagram of a surface is a simple combinatorial object, sometimes the non-existence of a diagram with required properties can be established by combinatorial methods. Combined with the representability result of the present paper this may be used to show the non-existence of a convex surface with certain properties in the complement of a Legendrian knot. If a convex surfaces with the same properties is known to exist for another Legendrian knot the two Legendrian types must be different. This method is out of the scope of the present paper and will be presented in a subsequent paper.

We also consider here in more detail embedded convex (in Giroux's sense) annuli in  $\mathbb{S}^3$  tangent to the contact structure along the boundary. Such annuli are the main building blocks of closed convex surfaces in  $\mathbb{S}^3$ . We discuss the following specific question: are the two boundary components of such an annulus always equivalent as Legendrian knots?

This question appears to be highly non-trivial. An attempt to answer it in the positive was made in manuscript [17] but a complete proof was not given. We believe that the answer is actually negative, but our attempt to find a *simple* counterexample has failed. In a number of examples that we tried the two boundary components of the annulus appeared to be Legendrian equivalent, and a Legendrian isotopy was easily found. Namely, the boundary components were transformed to each other by elementary moves preserving the complexity of the diagram (exchange moves).

We propose here an example of an annulus of the above mentioned type whose boundary components cannot be transformed to each other without using stabilizations. We conjecture that the two Legendrian knot types in our example are different.

*Remark 1.* Another use of rectangular diagrams of links comes from their relation to Floer homologies. As C. Manolescu, P. Ozsváth, and S. Sarkar show in [23] the definition of the knot Floer homology for links presented in the grid form can be given in purely combinatorial terms. Up to this writing, we are not aware of any useful interaction between rectangular diagrams of surfaces and algebraic theories. It would be interesting to see some.

The paper is organized as follows. In Section 2 we introduce the main subject of the paper, rectangular diagrams of surfaces, and other basic related objects. We show that every isotopy class of a surface can be presented by a rectangular diagram, but rectangular presentations of the boundary that will arise in this way satisfy certain restrictions. In Section 3 we discuss Legendrian links and graphs and their presentations by rectangular diagrams. They are used in the formulation and the proof of our main result—on the representability of convex surfaces by rectangular diagrams—which occupy Section 4. At the end of Section 4 we discuss the above mentioned conjecture about annuli with Legendrian boundary.

**Acknowledgement.** We are indebted to our anonymous referee for very careful reading of our paper, which has led to many clarifications in the text.

## 2. RECTANGULAR DIAGRAMS OF A SURFACE

**2.1. Definitions.** For any two distinct points  $x, y$ , say, of the oriented circle  $\mathbb{S}^1$  we denote by  $[x, y]$  the closed arc of  $\mathbb{S}^1$  with endpoints  $x, y$  such that  $\partial[x, y] = y - x$  if it is endowed with the orientation inherited from  $\mathbb{S}^1$ , see Fig. 1. By  $(x, y)$  we denote the corresponding open arc:  $(x, y) = [x, y] \setminus \{x, y\}$ .

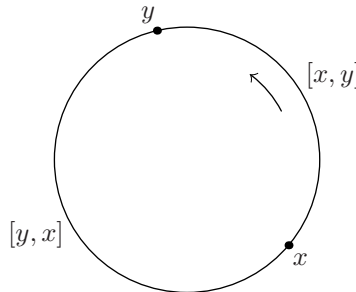


FIGURE 1. Intervals  $[x, y]$  and  $[y, x]$  on the oriented circle  $\mathbb{S}^1$

**Definition 1.** A *rectangle* in the 2-torus  $\mathbb{T}^2 = \mathbb{S}^1 \times \mathbb{S}^1$  is a subset of the form  $[\theta_1, \theta_2] \times [\varphi_1, \varphi_2]$ , where  $\theta_1 \neq \theta_2$ ,  $\varphi_1 \neq \varphi_2$ ,  $\theta_1, \theta_2, \varphi_1, \varphi_2 \in \mathbb{S}^1$ .

Two rectangles  $r_1, r_2$  are said to be *compatible* if their intersection satisfies one of the following:

- (1)  $r_1 \cap r_2$  is empty;
- (2)  $r_1 \cap r_2$  is a subset of vertices of  $r_1$ ;

(3)  $r_1 \cap r_2$  is a rectangle disjoint from the vertices of both rectangles  $r_1$  and  $r_2$ .

A *rectangular diagram of a surface* is a collection  $\Pi = \{r_1, \dots, r_k\}$  of pairwise compatible rectangles in  $\mathbb{T}^2$  such that every meridian  $\{\theta\} \times \mathbb{S}^1$  and every longitude  $\mathbb{S}^1 \times \{\varphi\}$  of the torus contains at most two free vertices, where by a *free vertex* we mean a point that is a vertex of exactly one rectangle from  $\Pi$ .

To represent such a diagram graphically, we draw  $\mathbb{T}^2$  as a square with identified opposite sides, so, some rectangles are cut into two or four pieces, see Fig. 2.

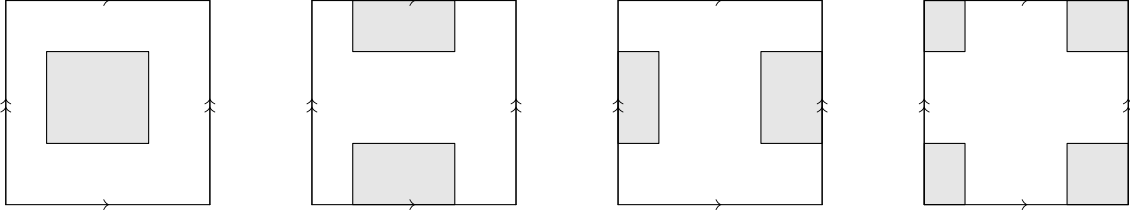


FIGURE 2. A rectangle in  $\mathbb{T}^2$

One can see that for any pair of compatible rectangles one of the following three mutually exclusive cases occurs:

- (1) the rectangles are disjoint;
- (2) the rectangles share 1, 2, or 4 vertices and are otherwise disjoint;
- (3) the rectangles have the form (possibly after exchanging them)  $r_1 = [\theta_1, \theta_2] \times [\varphi_1, \varphi_2]$ ,  $r_2 = [\theta_3, \theta_4] \times [\varphi_3, \varphi_4]$  with

$$[\theta_1, \theta_2] \subset (\theta_3, \theta_4), \quad [\varphi_3, \varphi_4] \subset (\varphi_1, \varphi_2).$$

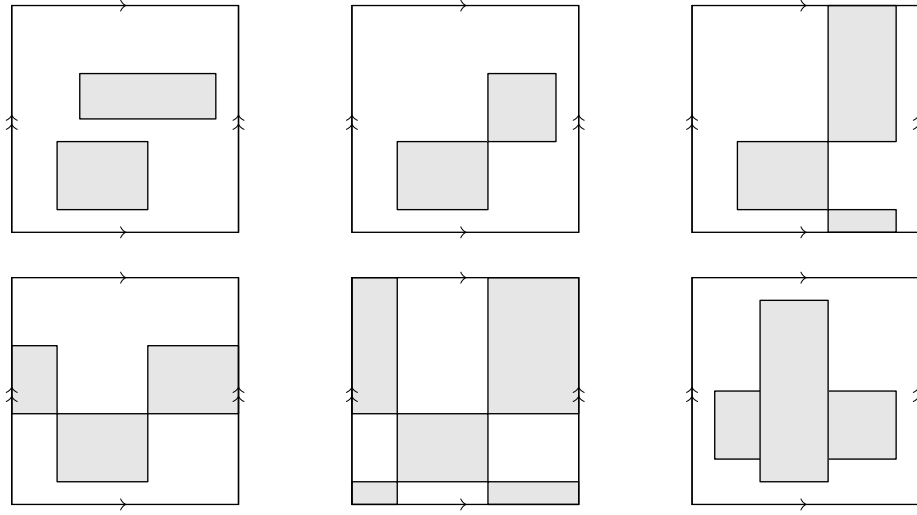


FIGURE 3. Compatible rectangles

In the latter case we draw  $r_1$  as if it passes over  $r_2$ , see Fig. 3.

An example of a rectangular diagram of a surface is shown in Fig. 4 on the left. The free vertices are marked by small circles.

**Definition 2.** By a *rectangular diagram of a link* we mean a finite set  $R$  of points in  $\mathbb{T}^2$  such that every meridian and every longitude of  $\mathbb{T}^2$  contains no or exactly two points from  $R$ . The points in  $R$  are referred to as *vertices of  $R$* .

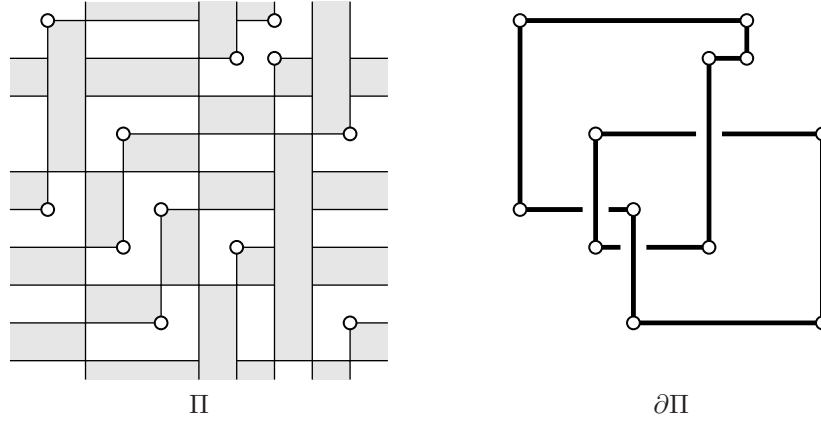


FIGURE 4. A rectangular diagram of a surface and its boundary

When  $R$  is presented graphically in a square, the vertical and horizontal straight line segments connecting two vertices of  $R$  will be called *the edges of  $R$* . Formally, an *edge* of  $R$  is a pair of vertices lying on the same longitude or meridian of  $\mathbb{T}^2$ . Such vertices are said *to be connected by an edge*, and this will have literal meaning in the pictures.

A rectangular diagram of a link  $R$  is said to be *connected* or to be a *rectangular diagram of a knot* if the vertices of  $R$  can be ordered so that any two consecutive vertices are connected by an edge.

A *connected component* of a rectangular diagram of a link is a non-empty subset that is a rectangular diagram of a knot.

**Definition 3.** Let  $\Pi$  be a rectangular diagram of a surface. The set of free vertices of  $\Pi$  will be called *the boundary of  $\Pi$*  and denoted by  $\partial\Pi$ .

It is readily seen that the boundary of a rectangular diagram of a surface is always a rectangular diagram of a link. In particular, for any rectangle  $r \subset \mathbb{T}^2$  the boundary  $\partial\{r\}$  of the diagram  $\{r\}$  is the set of vertices of  $r$ . It should not be confused with the boundary  $\partial r$  of the rectangle itself, which is understood in the conventional sense.

Fig. 4 shows a rectangular diagram of a surface (left) and its boundary (right) with edges added. The reason for drawing some edges passing over the others will be explained below.

**2.2. Cusps and pizza slices.** Here we introduce the class of topological objects (curves and surfaces) we will mostly deal with.

**Definition 4.** Let  $K$  be a piecewise smooth simple arc or simple closed curve in  $\mathbb{S}^3$  and  $p \in K$  a point distinct from the endpoints. We say that  $K$  has a *cusp* at the point  $p$  if  $K$  admits a local parametrization  $\gamma : (-1, 1) \rightarrow K$  such that

$$\lim_{t \rightarrow -0} \dot{\gamma} = - \lim_{t \rightarrow +0} \dot{\gamma} \neq 0, \quad \gamma(0) = p.$$

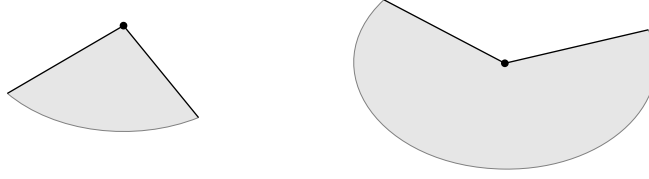
The curve  $K$  is called *cusp-free* if it has no cusps, and *cusped* if all singularities of  $K$  are cusps.

The links in  $\mathbb{S}^3$  that we consider will always be cusp-free.

**Definition 5.** We say that  $F \subset \mathbb{S}^3$  is a *surface with corners* if  $F$  is a subset of a 2-dimensional submanifold  $M \subset \mathbb{S}^3$  with (possibly empty) boundary such that:

- (1) the embedding  $M \hookrightarrow \mathbb{S}^3$  is regular and of smoothness class  $C^1$ ;
- (2)  $F$  is bounded in  $M$  by a (possibly empty) collection of mutually disjoint piecewise smooth cusp-free simple closed curves.

This definition simply means that surfaces we want to consider may have corners at the boundary, but in a broader sense than one usually means by saying ‘a manifold with corners’. Namely, the angle at a

FIGURE 5. Arbitrary angles from  $(0, 2\pi)$  are allowed at corners

corner can be arbitrary between 0 and  $2\pi$  (exclusive), not necessarily between 0 and  $\pi$  see Fig. 5. However, surfaces with corners are not allowed to spiral around a point at the boundary as shown in Fig. 6.

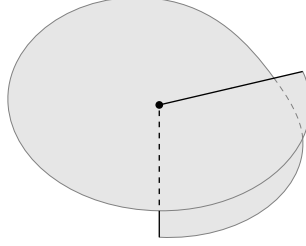


FIGURE 6. Spiralling around a boundary point is forbidden for a surface with corners

For future use we also need the following definition.

**Definition 6.** By a *pizza slice* centered at  $p \in \mathbb{S}^3$  we mean a disc that has the form  $F \cap \mathbb{B}_\varepsilon(p)$ , where  $F$  is a surface with corners such that  $p \in \partial F$ , and  $\mathbb{B}_\varepsilon(p)$  is a closed ball centered at  $p$  with small enough radius  $\varepsilon > 0$  such that  $\partial F$  has no singularities in  $\mathbb{B}_\varepsilon(p) \setminus \{p\}$  and  $\partial F \cap \mathbb{B}_\varepsilon(p)$  consists of a single arc. (The point  $p$  may or may not be a singularity of  $\partial F$ .)

For such a pizza slice we also say that it is *attached to the arc*  $\partial F \cap \mathbb{B}_\varepsilon(p)$ .

Two pizza slices  $\nabla_1, \nabla_2$  centered at the same point  $p \in \mathbb{S}^3$  are said to be *equivalent* if for small enough  $\varepsilon > 0$  the pizza slices  $\nabla'_i = \nabla_i \cap \mathbb{B}_\varepsilon(p)$ ,  $i = 1, 2$ , are attached to the same arc and for  $x \in \nabla_1$  we have  $d(x, \nabla_2) = o(d(x, p))$  ( $x \rightarrow p$ ), where  $d(\cdot, \cdot)$  denotes the distance function.

**2.3. 3D realizations of rectangular diagrams.** With every rectangular diagram of a link or a surface we associate an actual link or a surface, respectively, in  $\mathbb{S}^3$  as we now describe.

We represent  $\mathbb{S}^3$  as the join of two circles:

$$(1) \quad \mathbb{S}^3 = \mathbb{S}^1 * \mathbb{S}^1 = (\mathbb{S}^1 \times \mathbb{S}^1 \times [0, 1]) / ((\theta, \varphi, 0) \sim (\theta', \varphi, 0), (\theta, \varphi, 1) \sim (\theta, \varphi', 1)).$$

We also identify it with the unit sphere in  $\mathbb{R}^4$  as follows:

$$(\theta, \varphi, \tau) \mapsto (\cos(\pi\tau/2) \cos \varphi, \cos(\pi\tau/2) \sin \varphi, \sin(\pi\tau/2) \cos \theta, \sin(\pi\tau/2) \sin \theta).$$

The triple  $(\theta, \varphi, \tau)$  will be used as a coordinate system in  $\mathbb{S}^3$ . The two circles defined by  $\tau = 0$  and  $\tau = 1$  will be denoted by  $\mathbb{S}_{\tau=0}^1$  and  $\mathbb{S}_{\tau=1}^1$ , respectively.

**Definition 7.** By the *torus projection* of a subset  $X \subset \mathbb{S}^3$  we mean the image of  $X \setminus (\mathbb{S}_{\tau=0}^1 \cup \mathbb{S}_{\tau=1}^1)$  under the map  $\mathbb{S}^3 \setminus (\mathbb{S}_{\tau=0}^1 \cup \mathbb{S}_{\tau=1}^1) \rightarrow \mathbb{T}^2$  defined by  $(\theta, \varphi, \tau) \mapsto (\theta, \varphi)$ .

For a point  $v = (\theta, \varphi)$  in  $\mathbb{T}^2$  we denote by  $\hat{v}$  the image of the arc  $v \times [0, 1] \subset \mathbb{S}^1 \times \mathbb{S}^1 \times [0, 1]$  in  $\mathbb{S}^3 = \mathbb{S}^1 * \mathbb{S}^1$ .

**Definition 8.** Let  $R$  be a rectangular diagram of a link. By the *link associated with  $R$*  we mean the following union of arcs:  $\hat{R} = \bigcup_{v \in R} \hat{v}$ .

One can see that this union is indeed a collection of pairwise disjoint simple closed piecewise smooth curves. Moreover,  $\widehat{R}$  is a union of piecewise geodesic closed curves, which are cusp-free. One can also see that if  $R' \subset R$  is a connected component of  $R$ , then  $\widehat{R}'$  is a connected component of  $\widehat{R}$  and vice versa.

To get a conventional, planar picture of a link isotopic to  $\widehat{R}$  one cuts  $\mathbb{T}^2$  into a square and then join the vertices of  $R$  by edges, letting the vertical edges pass over the horizontal ones, see the right picture in Fig. 4. Finally, we remark that  $R$  is the torus projection of  $\widehat{R}$ , and  $\widehat{R}$  is the only link satisfying this property.

Cooking a surface out of a rectangular diagram of a surface is less visual, but the main principle is similar: the surface associated with a rectangular diagram of a surface should have the torus projection prescribed by the diagram. The surface associated with a rectangular diagram will be composed of discs associated with individual rectangles.

For a rectangle  $r = [\theta_1, \theta_2] \times [\varphi_1, \varphi_2] \subset \mathbb{T}^2$ , the image of  $r \times [0, 1]$  in  $\mathbb{S}^3$  under identifications (1) is the tetrahedron  $[\theta_1, \theta_2] * [\varphi_1, \varphi_2] \subset \mathbb{S}^1 * \mathbb{S}^1$ , which we denote by  $\Delta_r$ . We want to define  $\widehat{r}$  as a disc in  $\Delta_r$  with boundary  $\{\theta_1, \theta_2\} * \{\varphi_1, \varphi_2\}$  so that the union of such discs over all rectangles of a rectangular diagram of a surface yield a smoothly embedded surface. This can be done in numerous ways among which we choose one particularly convenient as it allows us to write down an explicit parametrization of  $\widehat{r}$  and behaves nicely in the respects addressed in Section 4.

We denote by  $h_r$  a bounded harmonic function on the interior  $\text{int}(r)$  of  $r$  that tends to 0 as  $\varphi$  tends to  $\varphi_1$  or  $\varphi_2$  while  $\theta \in (\theta_1, \theta_2)$  stays fixed, and tends to 1 as  $\theta$  tends to  $\theta_1$  or  $\theta_2$  while  $\varphi \in (\varphi_1, \varphi_2)$  stays fixed. Such a function exists and is unique, which follows from the Poisson integral formula and the uniformization theorem.

*Remark 2.* The function  $h_r$  admits an explicit presentation in terms of the Weierstrass elliptic function  $\wp(z) = \wp(z \mid \theta_2 - \theta_1, \mathbf{i}(\varphi_2 - \varphi_1))$  with half-periods  $(\theta_2 - \theta_1)$  and  $\mathbf{i}(\varphi_2 - \varphi_1)$ :

$$h_r(\theta, \varphi) = \frac{1}{\pi} \arg \frac{\wp(z_{\theta, \varphi}) - \wp(z_{\theta_2, \varphi_2})}{(\wp(z_{\theta, \varphi}) - \wp(z_{\theta_1, \varphi_2}))(\wp(z_{\theta, \varphi}) - \wp(z_{\theta_2, \varphi_1}))},$$

where  $z_{\theta, \varphi} = \theta - \theta_1 + \mathbf{i}(\varphi - \varphi_1)$ ,  $\theta_{1,2}$  and  $\varphi_{1,2}$  are assumed to be reals satisfying  $\theta_1 < \theta_2 < \theta_1 + 2\pi$ ,  $\varphi_1 < \varphi_2 < \varphi_1 + 2\pi$ .

**Definition 9.** We call the image in  $\mathbb{S}^3$  under identifications (1) of the closure of the following open disc in  $\mathbb{T}^2 \times [0, 1]$ :

$$(2) \quad \left\{ (v, \widetilde{h}_r(v)) ; v \in \text{int}(r) \right\}, \quad \text{where } \widetilde{h}_r(v) = (2/\pi) \cdot \arctan \sqrt{\tan(\pi h_r(v)/2)},$$

the tile associated with  $r$  and denote it by  $\widehat{r}$ .

Let  $\Pi$  be a rectangular diagram of a surface. We define the surface associated with  $\Pi$  to be the union  $\widehat{\Pi}$  of the tiles associated with rectangles from  $\Pi$ :  $\widehat{\Pi} = \bigcup_{r \in \Pi} \widehat{r}$ .

**Proposition 1.** Let  $\Pi$  be a rectangular diagram of a surface. Then  $\widehat{\Pi}$  is a surface with corners in  $\mathbb{S}^3$ , and we have  $\partial \widehat{\Pi} = \widehat{\partial \Pi}$ .

*Proof.* First consider a single rectangle  $r = [\theta_1, \theta_2] \times [\varphi_1, \varphi_2]$ . The function  $h_r$  can be extended continuously and smoothly to  $\partial r$  except at the vertices of  $r$ , where it jumps by  $\pm 1$ . The closure  $\Gamma$  of the graph of  $h_r$  is a smooth image of an octagon. Its boundary  $\partial \Gamma$  consists of four straight line segments parallel to the sides of  $r$  and another four straight line segments hanging over the vertices of  $r$ , see Fig. 7.

Along each of the latter four straight line segments,  $\Gamma$  is tangent to a helicoid that is independent of the size of  $r$  (i.e. of  $\theta_2 - \theta_1$  and  $\varphi_2 - \varphi_1$ ): the tangent plane to  $\Gamma$  at the point  $(\theta_i, \varphi_j, h)$ ,  $i, j \in \{1, 2\}$ ,  $h \in [0, 1]$ , is  $\ker(\cos(\pi h/2) d\varphi - (-1)^{i-j} \sin(\pi h/2) d\theta)$ . Tangency with a helicoid is a general property of the graphs of bounded harmonic functions on a polygon that are constant on each side of the polygon and have jumps at corners. Near each corner  $w_0 \in \mathbb{C}$  such a function  $h$  has a form  $h(w) = a + b \text{Arg}(w - w_0) + o(|w|)$ , where  $a, b \in \mathbb{R}$  and  $w$  is a complex coordinate in the plane. The tangency with a helicoid can even be shown to be of the second order.

By composing  $h_r$  with the map  $\zeta : x \mapsto (2/\pi) \cdot \arctan \sqrt{\tan(\pi x/2)}$ , which is a monotonic function  $[0, 1] \rightarrow [0, 1]$  such that  $\zeta(1-x) = 1 - \zeta(x)$  and  $\zeta'(0) = \zeta'(1) = \infty$ , we get the function  $\widetilde{h}_r$ , whose graph  $\widetilde{\Gamma}$

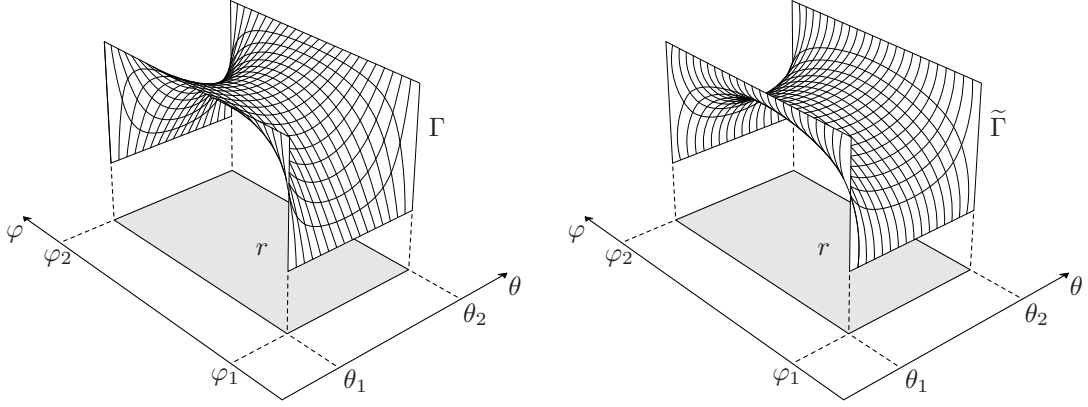


FIGURE 7. The graphs  $\Gamma$  and  $\tilde{\Gamma}$  of the functions  $h_r(\theta, \varphi)$  and  $\tilde{h}_r(\theta, \varphi)$ , respectively

is also a curved octagon with the same boundary as  $\Gamma$ , but now it has an additional property that the tangent plane to  $\tilde{\Gamma}$  is orthogonal to the  $(\theta, \varphi)$ -plane along the whole of the boundary  $\partial\tilde{\Gamma}$ . The specific choice of  $\zeta$  will play an important role in the sequel.

Identification (1) takes  $\tilde{\Gamma}$  to a disc with corners in  $\mathbb{S}^3$ , which is the tile  $\hat{r}$ . Fig. 8 shows a tile projected stereographically into  $\mathbb{R}^3$ . (The reader is alerted that the ‘coordinate grids’ in Fig. 7, which are added to visualize the surfaces, are not related to that in Fig. 8.) The boundary  $\partial\hat{r}$  has exactly two points at each of the circles  $\mathbb{S}_{\tau=0}^1$  and  $\mathbb{S}_{\tau=1}^1$ , and at these points the tangent plane to  $\hat{r}$  is orthogonal to the corresponding circle.

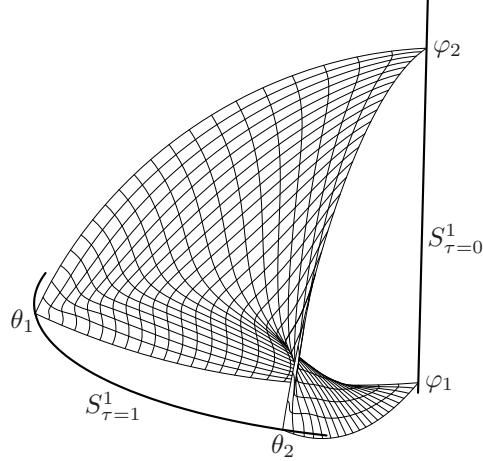


FIGURE 8. A tile

These points will be referred to as *the vertices of  $\hat{r}$* , and the four arcs of the form  $\hat{v}$ , where  $v \in \{\theta_1, \theta_2\} \times \{\varphi_1, \varphi_2\}$ , which form the boundary of  $\hat{r}$ , *the sides of  $\hat{r}$* .

By construction we also have the following.

**Lemma 1.** *The tile  $\hat{r}$  is tangent to the plane field*

$$(3) \quad \xi_- = \ker(\cos^2(\pi\tau/2) d\varphi - \sin^2(\pi\tau/2) d\theta)$$

*along the sides  $\widehat{(\theta_1, \varphi_1)}$  and  $\widehat{(\theta_2, \varphi_2)}$ , and to the plane field*

$$(4) \quad \xi_+ = \ker(\cos^2(\pi\tau/2) d\varphi + \sin^2(\pi\tau/2) d\theta)$$

*along the sides  $\widehat{(\theta_1, \varphi_2)}$  and  $\widehat{(\theta_2, \varphi_1)}$ .*



Let  $r_1$  and  $r_2$  be two compatible rectangles. If they are disjoint, then either the tiles  $\hat{r}_1$  and  $\hat{r}_2$  are disjoint or they share one or two vertices. In the latter case they have the same tangent plane at the common vertices.

If  $r_1$  and  $r_2$  share a vertex  $v$ , say, then  $\hat{r}_1$  and  $\hat{r}_2$  share a side, which is  $\hat{v}$ , and all other tiles are disjoint from  $\text{int}(\hat{v})$ . The tiles  $\hat{r}_1$  and  $\hat{r}_2$  approach  $\hat{v}$  from opposite sides and have the same tangent plane at each point of  $\hat{v}$ . Moreover, the intersection  $\hat{r}_1 \cap \hat{r}_2$  has the form  $\cup_{v \in r_1 \cap r_2} \hat{v}$ , where  $r_1 \cap r_2$  consists of common vertices of  $r_1$  and  $r_2$  (one, two, or four of them). Thus, the direction of the tangent plane to  $\hat{r}_1 \cup \hat{r}_2$  has no discontinuity at  $\hat{r}_1 \cap \hat{r}_2$ .

Figure 9 shows the preimages in  $\mathbb{T}^2 \times [0, 1]$  of two tiles sharing a single side, and the tiles themselves.

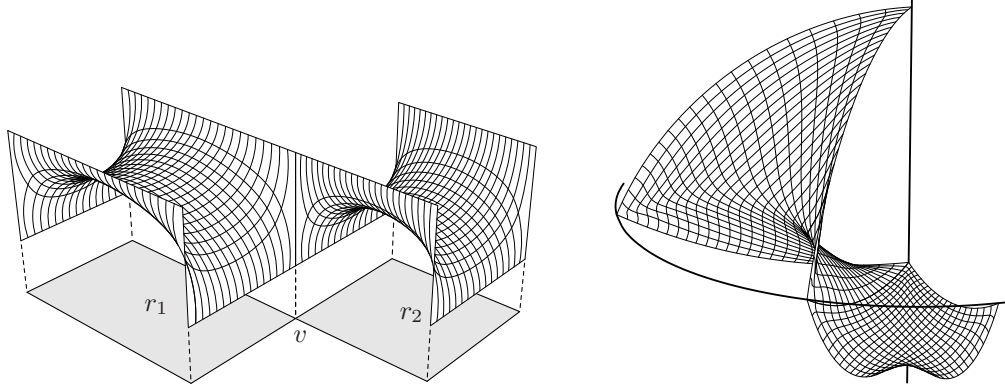


FIGURE 9. Two tiles sharing a side

Finally, if  $r = r_1 \cap r_2$  is a rectangle, then the tiles  $\hat{r}_1$  and  $\hat{r}_2$  are disjoint. Indeed, by construction, at the horizontal sides of  $r$  one of the functions  $h_{r_1}$ ,  $h_{r_2}$  vanishes whereas the other is strictly positive, and at the vertical sides of  $r$  one of these functions equals 1 and the other is strictly less than 1. Thus, we have  $h_{r_1}(x) \neq h_{r_2}(x)$  for all  $x \in \partial r$ , and, therefore, the inequality  $h_{r_1}(x) \neq h_{r_2}(x)$  also holds for all  $x \in r$  by the maximum principle for harmonic functions. Fig. 10 shows the relative position of the graphs of the functions  $\tilde{h}_{r_1}$  and  $\tilde{h}_{r_2}$  and the associated tiles in this case.

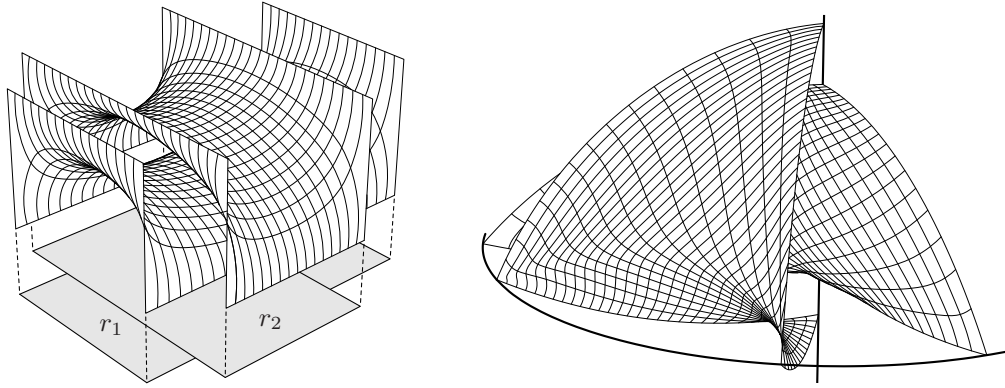


FIGURE 10. Two tiles corresponding to overlapping rectangles

Thus, in general, intersection of any two tiles  $\hat{r}_1$ ,  $\hat{r}_2$  of  $\hat{\Pi}$  bounds to the intersection of their boundaries, and the direction of the tangent plane to  $\hat{\Pi}$  is continuous on the whole of  $\hat{\Pi}$ . It remains to examine the boundary of  $\hat{\Pi}$  and to verify that no singularities other than corners occur at  $\partial\hat{\Pi}$ .

The boundary of each tile  $\widehat{r}$  consists of four arcs of the form  $\widehat{v}$ , where  $v$  is a vertex of  $r$ . If  $v$  is a vertex of two rectangles from  $\Pi$ , then two tiles of  $\widehat{\Pi}$  are attached to  $\widehat{v}$ , so, the interior of  $\widehat{v}$  is disjoint from  $\partial\widehat{\Pi}$ . Thus,  $\partial\widehat{\Pi}$  consists of all the arcs  $\widehat{v}$  such that  $v$  is a free vertex of  $\Pi$ . This implies  $\partial\widehat{\Pi} = \widehat{\partial\Pi}$ .

Let  $p$  be a point in  $\widehat{\Pi} \cap \mathbb{S}_{\tau=0}^1$ . It corresponds to a longitude of the torus  $\mathbb{T}^2$ . Let this longitude be  $\varphi = \varphi_0$  and denote it by  $\ell$ . The tiles having  $p$  as a vertex are associated with rectangles of the form  $[\theta_1, \theta_2] \times [\varphi_0, \varphi_1]$  or  $[\theta_1, \theta_2] \times [\varphi_1, \varphi_0]$ . Let  $r_1, \dots, r_m$  be all such rectangles.

For small enough  $\varepsilon > 0$ , the intersections  $\nabla_i = \widehat{r}_i \cap \mathbb{B}_\varepsilon(p)$  are all pizza slices, and the only our concern is what their union looks like.

Since the rectangles  $r_1, \dots, r_m$  are pairwise compatible, the arcs  $r_i \cap \ell$  have pairwise disjoint interiors. The last condition in the definition of a rectangular diagram of a surface guarantees that  $(\bigcup_{i=1}^m r_i) \cap \ell$  is either the whole of  $\ell$  or a single arc of the form  $[\theta', \theta''] \times \{\varphi_0\}$ .

In the former case, the union  $\bigcup_{i=1}^m \nabla_i$  is ‘the whole pizza’, i.e. a disc contained in the interior of  $\widehat{\Pi}$ . In the latter case, this union is a pizza slice with the angle  $\alpha \in (0, 2\pi)$ ,  $\alpha \equiv \theta'' - \theta' \pmod{2\pi}$ , at  $p$ .

The intersection of  $\widehat{\Pi}$  with the circle  $\mathbb{S}_{\tau=1}^1$  is considered similarly.  $\square$

*Remark 3.* Recovering a surface from a rectangular diagram of a surface as described above may look somewhat counterintuitive. Indeed, if  $r$  is a rectangle, the vertices of the tile  $\widehat{r}$  correspond to the sides of  $r$  and the sides of  $\widehat{r}$  to the vertices of  $r$ .

However, as we will see, presentation of surfaces by rectangular diagram is quite practical. In particular, the class of all surfaces of the form  $\widehat{\Pi}$  is such that each surface in it is uniquely recovered from its torus projection, whose closure is the union  $\bigcup_{r \in \Pi} r$ .

**2.4. Orientations.** Quite often one needs to endow surfaces and links with an orientation. Here is how to do this in the language of rectangular diagrams.

**Definition 10.** By an *oriented rectangular diagram of a link* we mean a pair  $(R, \epsilon)$  in which  $R$  is a rectangular diagram of a link and  $\epsilon$  is an assignment of ‘+’ or ‘−’ to every vertex so that the endpoints of every edge are assigned different signs. The vertices with ‘+’ assigned are referred to as *positive* and those with ‘−’ assigned *negative*. We also say that  $\epsilon$  is an *orientation* of  $R$ .

Every orientation  $\epsilon$  of a rectangular diagram of a link  $R$  defines an orientation of the link  $\widehat{R}$  by demanding that  $\tau$  increases on the oriented arc  $\widehat{v} \subset \widehat{R}$  whenever  $v$  is a positive vertex of  $R$  and decreases otherwise. One can readily see that this gives a one-to-one correspondence between orientations of a rectangular diagram of a link and those of the link associated with it.

*Remark 4.* From the combinatorial point of view oriented rectangular diagrams of links is the same thing as grid diagrams, with X’s in the latter corresponding to positive vertices and O’s to negative ones.

Now we introduce orientations for rectangular diagrams of surfaces.

The pair of functions  $(\theta, \varphi)$  is a local coordinate system in the interior of each tile. If two tiles  $t_1, t_2$ , say, share a side, then the orientations defined by this system in  $t_1$  and  $t_2$  disagree at  $t_1 \cap t_2$ , see Fig. 9. So, it is natural to specify an orientation of a rectangular diagram of a surface as follows.

**Definition 11.** An *oriented rectangular diagram of a surface* is a pair  $(\Pi, \epsilon)$  in which  $\Pi$  is a rectangular diagram of a surface and  $\epsilon$  is an assignment ‘+’ or ‘−’ to every rectangle in  $\Pi$  so that the signs assigned to any two rectangles sharing a vertex are different. The rectangles with ‘+’ assigned are then called *positive* and the others *negative*. The assignment  $\epsilon$  is referred to as an *orientation* of  $\Pi$ .

Like in the case of links, orientations of any rectangular diagram of a surface  $\Pi$  are put in one-to-one correspondence with orientations of the surface  $\widehat{\Pi}$  by demanding  $(\theta, \varphi)$  being a positively oriented coordinate pair in the tiles corresponding to positive rectangles, and negatively oriented coordinate pair in the tiles corresponding to negative rectangles. In particular,  $\Pi$  does not admit an orientation if and only if  $\widehat{\Pi}$  is a non-orientable surface.

In what follows, to simplify the notation, we omit an explicit reference to orientations.

**2.5. Framings.** We will need a slightly more general notion of a framing of a link than the one typically uses in knot theory.

**Definition 12.** Let  $L$  be a cusp-free piecewise smooth link in  $\mathbb{S}^3$ . By a *framing* of  $L$  we mean an isotopy class (relative to  $L$ ) of surfaces  $F$  with corners such that

- (1)  $F$  is a union of pairwise disjoint annuli  $A_1, \dots, A_k$ ;
- (2) for each  $i = 1, \dots, k$ , one of the connected components of  $\partial A_i$  is a component of  $L$  and the other is smooth and disjoint from  $L$ .

If  $f$  is a framing of a link  $L$  and  $F$  is a collection of annuli representing  $f$ , then we denote by  $L^f$  the link  $\partial F \setminus L$ . Roughly speaking,  $L^f$  is obtained from  $L$  by shifting along the framing  $f$ . If  $L$  is oriented, then  $L^f$  is assumed to be oriented coherently with  $L$ .

We also denote by  $\langle f \rangle$  the linking number  $\text{lk}(L, L^f)$ , which is clearly an invariant of  $f$ . If  $L$  is a smooth knot then framings  $f$  of  $L$  are classified by  $\langle f \rangle \in \mathbb{Z}$  (which is independent on the orientation of the knot).

But if  $L$  has singularities, a framing contains more information. Indeed, at a singularity of  $L$ , the tangent plane to any surface  $F$  with corners such that  $L \subset \partial F$  is prescribed by  $L$ . So, it cannot be changed by an isotopy of  $F$  within the class of surfaces with corners.

The surface  $F$  can approach such a singularity from two sides. Formally, this means that if  $p$  is a singularity of  $\partial F$  and  $\gamma$  is an arc of the form  $\partial F \cap \mathbb{B}_\varepsilon(p)$  with small enough  $\varepsilon > 0$ , then there are two equivalence classes of pizza slices attached to  $\gamma$ , and the one that the surface  $F$  realizes is an invariant of the framing.

Let a framing  $f_0$  of  $L$  be fixed. If  $f$  is another framing of  $L$ , then the twist of  $f$  relative to  $f_0$  along any arc connecting two singularities of  $\partial F$  is a multiple of  $\pi$  and is also a topological invariant of  $f$ .

Clearly, these invariants determine the framing, and there are some obvious restrictions on them, which we need not to discuss.

If  $L' \subset L$  is a sublink, then the restriction  $f|_{L'}$  of a framing  $f$  is defined in the obvious way. Clearly, any framing of  $L$  is defined uniquely by its restriction to every connected component of  $L$ .

**Definition 13.** If  $F$  is a surface with corners we call the framing of  $\partial F$  defined by a collar neighborhood of  $\partial F$  the *boundary framing induced by  $F$* .

If  $L$  is a sublink of  $\partial F$ , where  $F$  is a surface then we denote by  $L^F$  any link contained in  $F$  such that  $L \cup L^F$  bounds a collar neighborhood of  $L$  in  $F$ .

**Definition 14.** Let  $R$  be a rectangular diagram of a link. By a *framing* of  $R$  we mean an ordering in each pair of vertices of  $R$  forming an edge of  $R$ .

For specifying a framing of a rectangular diagram of a link in a picture we proceed as follows. For every edge  $\{v_1, v_2\}$ , we draw the arc  $[v_1, v_2]$  if  $v_2 > v_1$  in the given framing and the arc  $[v_2, v_1]$  if  $v_1 > v_2$ . Here by  $[v_1, v_2]$  we mean  $[\theta_1, \theta_2] \times \{\varphi_0\} \subset \mathbb{T}^2$  if  $\{v_1, v_2\} = \{\theta_1, \theta_2\} \times \{\varphi_0\}$  is a horizontal edge and  $\{\theta_0\} \times [\varphi_1, \varphi_2]$  if  $\{v_1, v_2\} = \{\theta_0\} \times \{\varphi_1, \varphi_2\}$  is a vertical one. The arcs are assumed to be drawn on  $\mathbb{T}^2$ , so in the actual planar picture some of these arcs get cut into two pieces, see Fig. 11. As always, we draw

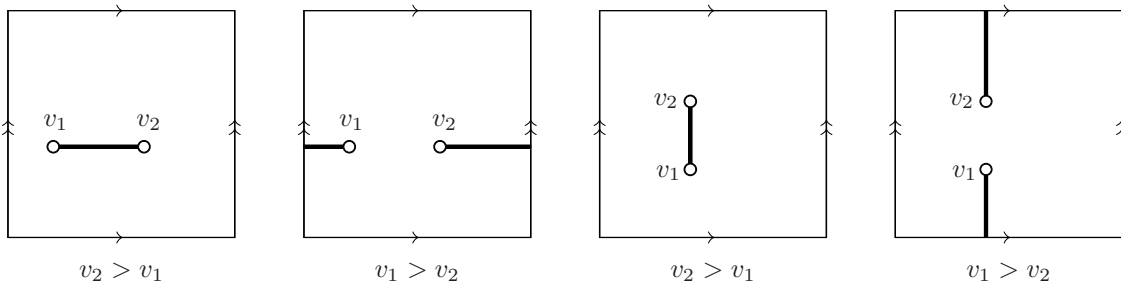


FIGURE 11. Specifying a framing in the picture of a rectangular diagram of a link

vertical arcs over horizontal ones. The right picture in Fig. 12 shows an example of a framed rectangular diagram of a link.

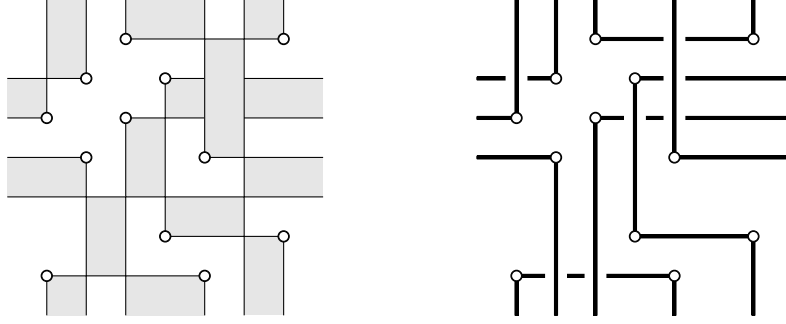


FIGURE 12. A rectangular diagram of a surface and its boundary with boundary framing

By definition, any rectangular diagram of a link supports only finitely many framings. They encode framings of the corresponding link in  $\mathbb{S}^3$  that are not ‘twisted too much’. We now define them formally.

**Definition 15.** Let  $R$  be a rectangular diagram of a link. A framing of  $\hat{R}$  is called *admissible* if it can be presented by a surface  $F$  tangent to one of the plane fields  $\xi_{\pm}$  defined by (3) and (4) at every point  $p \in \hat{R}$ .

With every admissible framing of  $\hat{R}$  we associate (in general, non-uniquely) a framing of  $R$  as follows.

Let  $F$  be a union of annuli that represents an admissible framing  $f$  of  $\hat{R}$  such that at every point  $q \in \hat{R}$  the surface  $F$  is tangent to  $\xi_+$  or  $\xi_-$ . Let  $p$  be a point from  $\hat{R} \cap (\mathbb{S}_{\tau=0}^1 \cup \mathbb{S}_{\tau=1}^1)$ . The tangent plane to  $F$  at  $p$  is orthogonal to the corresponding  $\mathbb{S}^1$  since so are  $\xi_{\pm}$ .

The intersection of  $F$  with a small ball  $\mathbb{B}_{\varepsilon}(p)$  is a pizza slice, which is equivalent to one of the form  $[v_1, v_2] \times [0, \varepsilon] / \sim$  or  $[v_1, v_2] \times [1 - \varepsilon, 1] / \sim$  (depending on whether  $p \in \mathbb{S}_{\tau=0}^1$  or  $p \in \mathbb{S}_{\tau=1}^1$ ), where  $\{v_1, v_2\}$  is the edge of  $R$  corresponding to  $p$ , and the equivalence  $\sim$  is given by (1). We denote the pizza slice  $F \cap \mathbb{B}_{\varepsilon}(p)$  by  $\nabla_p$ . The framing of  $R$  associated with  $f$  is defined on the edge  $\{v_1, v_2\}$  as  $v_2 > v_1$ .

**Proposition 2.** For a generic  $R$ , the construction above defines a one-to-one correspondence between admissible framings of  $\hat{R}$  and framings of  $R$ . In general, this correspondence is one-to-many.

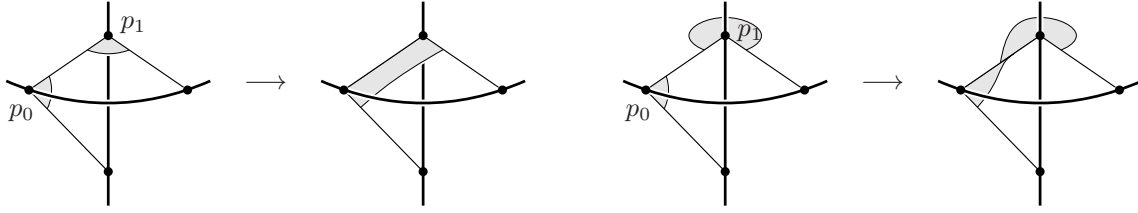
*Proof.* Clearly, we can recover the equivalence classes of the pizza slices  $\nabla_p$  from the corresponding framing of  $R$ , since the only information carried by the pizza slice  $\nabla_p$  is from which side it approaches the link  $\hat{R}$ . Namely, let  $p \in \mathbb{S}_{\tau=0}^1$  and let  $\{v_1, v_2\}$  be the corresponding horizontal edge. Then  $\nabla_p$  is equivalent either to  $[v_1, v_2] \times [0, \varepsilon] / \sim$  or to  $[v_2, v_1] \times [0, \varepsilon] / \sim$ , and a choice of one of this options is precisely the information recorded in the framing of  $R$ . Similarly for vertical edges.

The point now is that, for an admissible framing  $f$ , the equivalence classes of  $\nabla_p$ ’s define  $f$  completely. Indeed, let  $v$  be a vertex of  $R$  and  $p_0 \in \mathbb{S}_{\tau=0}^1$ ,  $p_1 \in \mathbb{S}_{\tau=1}^1$  the endpoints of  $\hat{v}$ . At  $p_i$ ,  $i = 0, 1$ , the tangent plane to  $F$  is orthogonal to  $\mathbb{S}_{\tau=i}^1$ , and the framing of  $R$  associated with  $f$  prescribes from which side the surface  $F$  approaches  $\hat{R}$ .

When  $q$  traverses  $\hat{v}$  the planes  $\xi_+(q)$  and  $\xi_-(q)$  rotate around  $\hat{v}$  by  $-\pi/2$  and  $\pi/2$ , respectively. Which way the tangent plane to  $F$  must rotate is determined by  $\nabla_{p_0}$  and  $\nabla_{p_1}$ , see Fig. 13. So, the framing  $f$  is recovered uniquely.

The only possible reason for the correspondence between framings of  $R$  and admissible framings of  $\hat{R}$  to not be a bijection is a situation when not all points in  $\hat{R} \cap (\mathbb{S}_{\tau=0}^1 \cup \mathbb{S}_{\tau=1}^1)$  are singularities of  $\hat{R}$ . This occurs when some edges of  $R$  have ‘length’  $\pi$ , which generically does not happen.

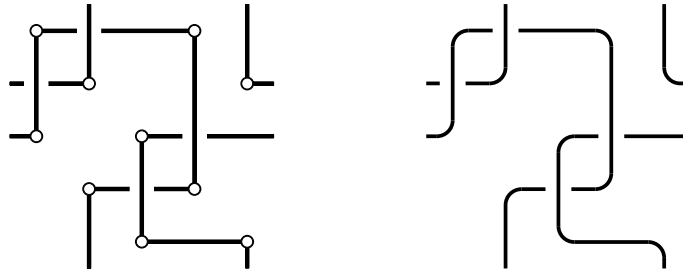
If this does happen, then the tangent plane to a surface representing  $f$  can rotate freely around  $\hat{R}$  at any point  $p \in \hat{R} \cap (\mathbb{S}_{\tau=0}^1 \cup \mathbb{S}_{\tau=1}^1)$  that is not a singularity of  $\hat{R}$ , so when such a surface is required to be tangent to  $\xi_{\pm}$  this does not necessarily prescribe from which side it should approach  $\hat{R}$  near  $p$ .  $\square$

FIGURE 13. Recovering an admissible framing from the pizza slices  $\nabla_p$ 

In the sequel we will assume that all rectangular diagrams of links that we consider are generic, and make no distinction between a framing of a diagram and an admissible framing of the corresponding link.

An obvious but important thing to note here is the following

**Approximation Principle.** *If  $(R, f)$  is a framed rectangular diagram of a link and  $D$  is the picture of  $(R, f)$  obtained as described right after Definition 14, then by smoothing  $D$  near the vertices of  $R$  we obtain the torus projection of a link of the form  $\widehat{R}^f$ , in which the indication of passing over and under at the crossings corresponds to the relative position of the arcs in the  $\tau$ -direction: the one with greater  $\tau$  is overcrossing, see Fig. 14.*

FIGURE 14. A framed rectangular diagram  $(R, f)$  and the torus projection of  $\widehat{R}^f$ 

The principle also works in the other way. If  $L \subset \mathbb{S}^3$  is a link disjoint from the circles  $\mathbb{S}_{\tau=0,1}^1$ , then a rectangular diagram of a link  $R$  such that  $\widehat{R}$  is isotopic to  $L$  can be obtained by approximating the torus projection of  $L$  by the picture of a framed rectangular diagram of a link.

If  $\Pi$  is a rectangular diagram of a surface, then  $\widehat{\Pi}$  is tangent to  $\xi_+$  or  $\xi_-$  at every point of the boundary. This together with Approximation Principle implies the following.

**Proposition 3.** *Let  $\Pi$  be a rectangular diagram of a surface and  $R = \partial\Pi$ . The boundary framing on  $\widehat{R}$  induced by  $\widehat{\Pi}$  is admissible.*

The picture of the corresponding framing of  $R$  is obtained by connecting each pair of vertices of  $R$  forming an edge by an arc in  $\mathbb{T}^2$  covered by the boundaries of the rectangles from  $\Pi$ , see Fig. 12.

**2.6. Thurston–Bennequin numbers.** Thurston–Bennequin number is a classical invariant of Legendrian links [1]. There are two Legendrian links associated with every rectangular diagram  $R$  (see [28, 6] and also Section 3 below<sup>1</sup>), and their Thurston–Bennequin numbers can be computed from  $R$  without any reference to the associated Legendrian links as we now describe.

Let  $R$  be a(n oriented) rectangular diagram of a link. By  $R^\nearrow$  we denote a diagram obtained from  $R$  by a small shift in the  $(1, 1)$ -direction, i.e. a diagram of the form

$$\{(\theta + \varepsilon, \varphi + \varepsilon) ; (\theta, \varphi) \in R\},$$

<sup>1</sup>The fact that arc-presentations ‘are Legendrian’ was mentioned by W. Menasco to the first present author already in 2003 and has been popularized since then

where  $\varepsilon > 0$  is so small that, whenever  $(\theta_0, \varphi_0)$  is a vertex of  $R$ , there are no vertices of  $R$  in the following four regions:

$$\theta_0 - \varepsilon \leq \theta < \theta_0, \quad \theta_0 < \theta \leq \theta_0 + \varepsilon, \quad \varphi_0 - \varepsilon \leq \varphi < \varphi_0, \quad \varphi_0 < \varphi \leq \varphi_0 + \varepsilon.$$

If  $R$  is oriented, then  $\widehat{R}^{\nearrow}$  inherits the orientation from  $R$ .

Similarly we define  $\widehat{R}^{\nwarrow}$  by using a shift in the  $(-1, 1)$ -direction.

**Definition 16.** Let  $R$  be an oriented diagram of a link. By the *Thurston–Bennequin numbers* of  $R$  we mean the following two linking numbers:

$$\text{tb}_+(R) = \text{lk}(\widehat{R}, \widehat{R}^{\nearrow}), \quad \text{tb}_-(R) = -\text{lk}(\widehat{R}, \widehat{R}^{\nwarrow}).$$

These numbers do not change if the orientation of  $R$  is reversed. So, if  $\widehat{R}$  is a knot, then the numbers  $\text{tb}_{\pm}(R)$  do not depend on the orientation of  $R$ , and we can speak about Thurston–Bennequin numbers of  $R$  even if  $R$  is not oriented.

**Proposition 4.** (i) Let  $R$  be an oriented rectangular diagram of a link and  $F$  a surface with corners in  $\mathbb{S}^3$  such that  $\partial F \supset \widehat{R}$ . If  $F$  is tangent to the plane field  $\xi_+$  defined by (4) (respectively,  $\xi_-$  defined by (3)) at all points of  $\widehat{R}$ , then  $\text{lk}(\widehat{R}, \widehat{R}^F)$  is equal to  $\text{tb}_+(R)$  (respectively, to  $-\text{tb}_-(R)$ ).

(ii) The following equality holds

$$(5) \quad \text{tb}_+(R) + \text{tb}_-(R) = -|R|/2,$$

where  $|R|$  denotes the number of vertices in  $R$ .

(iii) The set

$$\{\langle f \rangle ; f \text{ is a framing of } R\}$$

coincides with  $[\text{tb}_+(R), -\text{tb}_-(R)] \cap \mathbb{Z}$ .

*Proof.* Claim (i) follows from the fact that  $\widehat{R}^{\nearrow}$  (respectively,  $\widehat{R}^{\nwarrow}$ ) is obtained from  $\widehat{R}$  by a small shift in a direction transverse to  $\xi_+$  (respectively, to  $\xi_-$ ).

When  $p$  traverses an arc of the form  $\widehat{v}$ , where  $v \in R$ , the plane  $\xi_+(p)$  rotates relative to the plane  $\xi_-(p)$  by the angle  $-\pi$ . This implies Claim (ii).

We also see, that  $\langle f \rangle$  is maximized (respectively, minimized) over all admissible framings of  $\widehat{R}$  if it can be presented by a surface with corners  $F$  such that  $\widehat{R} \subset \partial F$  and  $F$  is tangent to  $\xi_-$  (respectively, to  $\xi_+$ ) along  $\widehat{R}$ . Thus  $\langle f \rangle \in [\text{tb}_+(R), -\text{tb}_-(R)]$  for any admissible framing  $f$ .

Let  $n = |R|/2$  and  $k \in [0, n] \cap \mathbb{Z}$ . Define a framing  $f_k$  as follows. For each horizontal edge  $\{v_-, v_+\}$  of  $R$  with  $v_-$  the negative vertex and  $v_+$  the positive one, we put  $v_+ > v_-$ . Do the same for  $k$  arbitrarily chosen vertical edges. For the remaining  $(n - k)$  vertical edges put the opposite:  $v_- > v_+$ .

Let  $F$  be a surface representing the corresponding admissible framing of  $\widehat{R}$ . There will be  $2k$  arcs of the form  $\widehat{v}$ ,  $v \in R$ , along which  $F$  is tangent to  $\xi_-$  and  $2(n - k)$  such arcs along which  $F$  is tangent to  $\xi_+$ . This implies  $\langle f_k \rangle = \text{tb}_+ + k$ . So, any integer in the interval  $[\text{tb}_+(R), -\text{tb}_-(R)]$  can be realized by  $\langle f \rangle$  for a framing  $f$  of  $R$ , which completes the proof of Claim (iii).  $\square$

**2.7. Which isotopy classes of surfaces can be presented by rectangular diagrams?** The following is a combinatorial definition of the relative Thurston–Bennequin number. The latter appears, e.g. in [19].

**Definition 17.** Let  $R$  be an oriented rectangular diagram of a link and  $F \subset \mathbb{S}^3$  a surface (which can be more general than a surface with corners) whose boundary contains  $\widehat{R}$ . By the *Thurston–Bennequin numbers of  $R$  relative to  $F$*  we call

$$\text{tb}_+(R; F) = \text{tb}_+(R) - \text{lk}(\widehat{R}, \widehat{R}^F), \quad \text{tb}_-(R; F) = \text{tb}_-(R) + \text{lk}(\widehat{R}, \widehat{R}^F).$$

Again, if  $R$  has a single connected component, then the numbers  $\text{tb}_{\pm}(R; F)$  are independent of the orientation of  $R$ .



**Theorem 1.** *Let  $R$  be a rectangular diagram of a link and let  $F$  be a compact surface in  $\mathbb{S}^3$  such that each connected component of  $\widehat{R}$  is either disjoint from  $F$  or contained in  $\partial F$ . Then a rectangular diagram of a surface  $\Pi$  such that  $\widehat{\Pi}$  is isotopic to  $F$  relative to  $\widehat{R}$  exists if and only if any connected component  $K \subset R$  such that  $\widehat{K} \subset \partial F$ , has non-positive Thurston–Bennequin numbers relative to  $F$ :*

$$(6) \quad \text{tb}_+(K, F) \leq 0, \quad \text{tb}_-(K, F) \leq 0.$$

In this theorem  $F$  is not necessarily assumed to be a surface with corners in the sense of Definition 5, and is allowed to have more general singularities at the boundary, both initially and during the isotopy. This allows to rotate it freely around  $\partial F$ , even near the singularities of  $\partial F$ .

*Proof.* First, we show that condition (6) is necessary. Let  $\Pi$  be a rectangular diagram of a surface and  $K$  a connected component of  $\partial \Pi$ . By Proposition 3 the boundary framing of  $K$  induced by  $\widehat{\Pi}$  is admissible.

Therefore, by Proposition 4 for any connected component  $K \subset R$  we have

$$\text{lk}(\widehat{K}, \widehat{K}^F) \in [\text{tb}_+(K), -\text{tb}_-(K)],$$

which is equivalent to (6).

Now assume that (6) holds for any component of  $\widehat{R} \cap \partial F$ . We will use Lemma 2 and Proposition 5 proven below.

The link  $\partial F$  can have connected components disjoint from  $\widehat{R}$ . By Lemma 2 we can isotop  $F$  keeping  $\widehat{R}$  fixed so that  $\partial F \setminus \widehat{R}$  will have the form  $\widehat{R}'$  for some rectangular diagram of a link  $R'$ . Moreover, we can ensure that the restriction of the boundary framing induced by  $F$  to any connected component  $\widehat{K} \subset \widehat{R}'$  is admissible by making  $\text{tb}_+(K)$  and  $\text{tb}_-(K)$  smaller than  $\text{lk}(\widehat{K}, \widehat{K}^F)$  and  $-\text{lk}(\widehat{K}, \widehat{K}^F)$ , respectively.

Thus, we may assume without loss of generality that  $\widehat{R}$  contains  $\partial F$  (we achieve this by replacing  $R$  with  $R \cup R'$ ). We can now isotop  $F$  by altering it only in a small neighborhood of  $\partial F$  so that  $F$  will become tangent either to  $\xi_+$  or to  $\xi_-$  at every point of  $\partial F$ .

Application of Proposition 5 with  $\widehat{X}_1 = \partial F$  and  $X_2 = R \setminus X_1$  completes the proof.  $\square$

**Lemma 2.** *Let  $R$  be a rectangular diagram of a link,  $L$  a link disjoint from  $\widehat{R}$ , and  $k$  an integer. Then there exists a rectangular diagram of a link  $R'$  such that*

- (1) *the link  $\widehat{R}'$  is isotopic to  $L$  relative to  $\widehat{R}$ ;*
- (2) *for any connected component  $K$  of  $R'$  we have  $\text{tb}_+(K) < k$  and  $\text{tb}_-(K) < k$ .*

*Proof.* To show the existence of  $R'$  without the restrictions on the Thurston–Bennequin numbers we follow the Approximation Principle with a slight modification that now we should avoid intersections with the given link  $\widehat{R}$  already given in the ‘rectangular’ form.

First, we perturb  $L$  slightly to make it disjoint from both circles  $\mathbb{S}_{\tau=0,1}^1$ . We may also ensure that the torus projection  $P$  of  $L$  has only double transverse self-intersections.

The torus projection of the link  $\widehat{R}$  is  $R$ . The torus projection  $P$  is disjoint from this set, since  $L$  is disjoint from  $\widehat{R}$ . Let  $\varepsilon$  be the distance between  $R$  and  $P$ .

We can now approximate  $P$  by a framed rectangular diagram of a link  $R'$  in the  $\varepsilon$ -neighborhood of  $P$ . By a small perturbation if necessary we can achieve that the edges of  $R'$  do not appear on the same longitudes or meridians as the edges of  $R$ . The link  $\widehat{R}'$  will be isotopic to  $L$  relative to  $\widehat{R}$ , see Fig. 15. (The framing that  $R'$  comes with plays no role in the sequel and should be discarded.)

Now if some of the Thurston–Bennequin numbers of connected components of  $R'$  are too large, we apply stabilizations to  $R'$ . Recall (see [5, 6]) that a *stabilization* of a rectangular diagram is a replacement of a vertex  $v_0$ , say, by three vertices  $v_1, v_2, v_3$  such that

- (1)  $v_0, v_1, v_2, v_3$  are vertices of a square  $s$  of the form  $[\theta_1, \theta_2] \times [\varphi_1, \varphi_2]$ ;
- (2) the square  $s$  is so small that there are no other vertices of the diagram inside the regions  $(\theta_1, \theta_2) \times \mathbb{S}^1$  and  $\mathbb{S}^1 \times (\varphi_1, \varphi_2)$  and there are exactly two vertices at the boundary of each.

We distinguish between *type I* and *type II* stabilizations as shown in Fig. 16. Type I stabilizations preserve  $\text{tb}_+$  and drop  $\text{tb}_-$  by 1. Type II stabilizations preserve  $\text{tb}_-$  and drop  $\text{tb}_+$  by 1. So, by applying

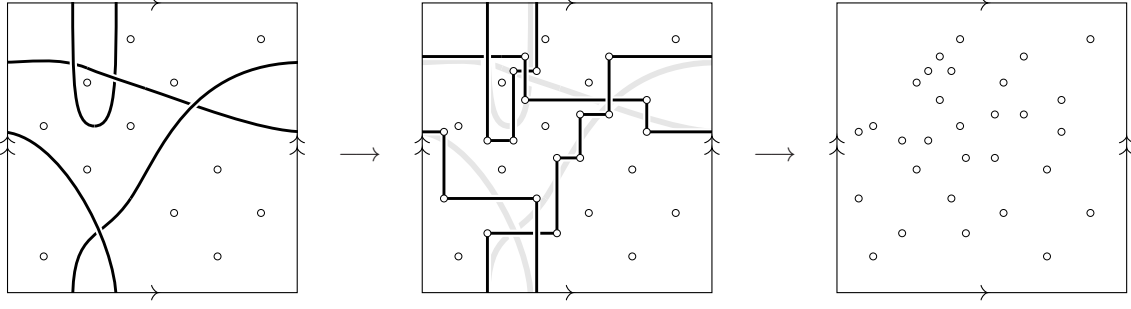


FIGURE 15. Approximating a torus projection of a link in the complement of  $\widehat{R}$  by a framed rectangular diagram of a link

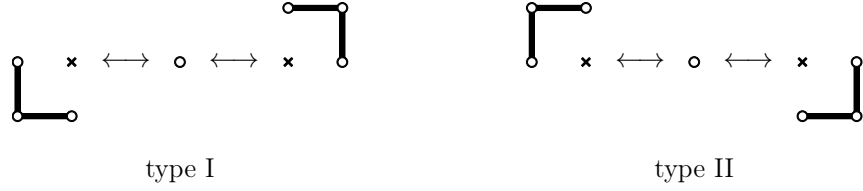


FIGURE 16. Types of stabilizations and destabilizations

sufficiently many stabilizations of appropriate types we make the Thurston–Bennequin numbers of all the components of  $R'$  smaller than the given  $k$ .  $\square$

For any finite subset  $X \subset \mathbb{T}^2$ , we will use notation  $\widehat{X}$  in the same sense as for rectangular diagrams:

$$\widehat{X} = \bigcup_{v \in X} \widehat{v}.$$

If  $X$  is not a rectangular diagram of a link, then  $\widehat{X}$  is not a link, but  $\widehat{X}$  is always a graph, i.e. a 1-dimensional CW-complex.

The following statement will be given in greater generality than necessary to establish Theorem 1. It will be used in full generality later in the proof of Theorem 2.

**Proposition 5.** *Let  $F$  be a surface with corners, and  $X_1, X_2$  two disjoint finite subsets of  $\mathbb{T}^2$ . Suppose that they satisfy the following conditions:*

- (1) *the graph  $\widehat{X}_1$  contains  $\partial F$ ;*
- (2)  *$F \cap \widehat{X}_2 \subset \widehat{X}_1$ ;*
- (3)  *$F$  contains  $\widehat{X}_1$ ;*
- (4)  *$F$  is tangent either to  $\xi_+$  or to  $\xi_-$  at all points of  $\widehat{X}_1$ .*

*Then there exists a rectangular diagram of a surface  $\Pi$  and an isotopy relative to  $\widehat{X_1 \cup X_2}$  taking  $F$  to  $\widehat{\Pi}$  such that the tangent plane to the surface remains constant at any point from  $\widehat{X}_1$  during the isotopy.*

The proof of this statement occupies the rest of this section.

*Proof.* We will be using the open book decomposition of  $\mathbb{S}^3$  with the binding circle  $\mathbb{S}_{\tau=0}^1$  and pages  $\mathcal{P}_\theta = \{\theta\} * \mathbb{S}^1 \subset \mathbb{S}^1 * \mathbb{S}^1$ ,  $\theta \in \mathbb{S}^1$ .

The sought-for diagram  $\Pi$  and an isotopy from  $F$  to  $\widehat{\Pi}$  will be constructed in four steps. At each step, we apply an isotopy to  $F$ , and the result will still be denoted by  $F$ . At the end we will have  $F = \widehat{\Pi}$ . Every isotopy is silently assumed to be fixed at  $\widehat{X_1 \cup X_2}$  and to have identity differential at  $\widehat{X}_1$  at every moment. One can see that all modification of  $F$  described below can be made so as to comply with



this restriction. Roughly speaking, the surface near  $\widehat{X}_1$  is already ‘good enough’ and doesn’t need to be altered there.

*Step 1.* We perturb  $F$  slightly to make it transverse to the binding circle, and so that the following conditions hold:

- (1) the restriction of the (multi-valued) function  $\theta$  to  $F \setminus \mathbb{S}_{\tau=0}^1$  has only finitely many critical points, and each page  $\mathcal{P}_\theta$  contains at most one of them;
- (2) each critical point of  $\theta|_{F \setminus \mathbb{S}_{\tau=0}^1}$  is a local maximum, a local minimum, or a multiple saddle (including those at the boundary, see explanations below);
- (3) strict local extrema of  $\theta|_{F \setminus \mathbb{S}_{\tau=0}^1}$  do not occur at  $\mathbb{S}_{\tau=1}^1$  (non-strict local extrema can occur at  $\partial F$ , they are not critical points);
- (4) any arc of the form  $\widehat{v}$ , where  $v \in \mathbb{T}^2$ , containing a local extremum of  $\theta|_{F \setminus \mathbb{S}_{\tau=0}^1}$  has no other tangency point with  $F$ ;
- (5) if  $p_1$  and  $p_2$  are two points of  $F$  at which  $\theta|_{F \setminus \mathbb{S}_{\tau=0}^1}$  has a local extremum, then the values of the coordinate  $\varphi$  at  $p_1$  and  $p_2$  are different.

All this is achieved by a generic arbitrarily small perturbation of  $F$ .

Some explanations are in order. Recall that throughout the paper we deal with surfaces with corners, whose smoothness class is only supposed to be  $C^1$ . So, when we speak about (multiple) saddle critical points we mean by that only the topological type of the singularity of the level line foliation.

Namely, let  $\theta_0$  be the value of  $\theta$  at such a singularity  $p$ , say. Assume that  $p$  is an interior point of  $F$ . In a small neighborhood of  $p$  the level line  $\theta|_F = \theta_0$  must be a star graph and the sign of  $(\theta|_F(q) - \theta_0)$  must change whenever  $q$  crosses any of its ‘legs’. The number of these legs is even and equals  $2(k+1)$ , where  $k$  is the *multiplicity* of the saddle. We put no restriction on the angle between the legs at  $p$ , and allow  $k$  to be zero.

By saying that  $p$  is a boundary (multiple) saddle we mean that it becomes a (multiple) saddle after a small extension of  $F$  beyond  $\partial F$ , which must exist by the definition of a surface with corners. Figs. 17 and 18 show a few examples of how the level line foliation may look like near an interior or boundary multiple saddle.

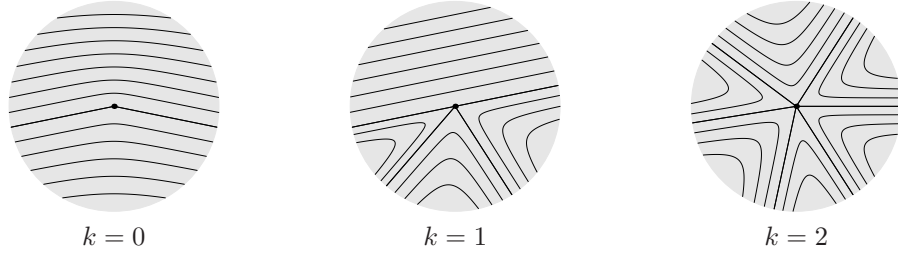


FIGURE 17. Examples of multiple saddles

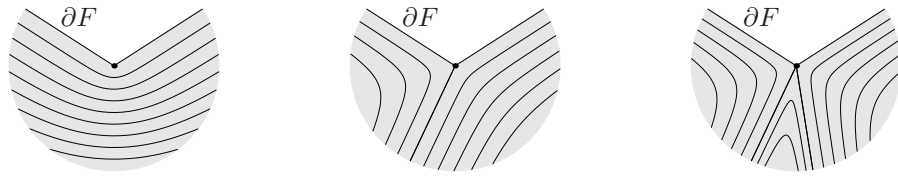


FIGURE 18. Examples of multiple saddles at the boundary

The reader may wonder why we allow multiple saddles for  $\theta|_{F \setminus \mathbb{S}_{\tau=0}^1}$  with other multiplicities than 1. This is because  $F$  and the tangent plane to  $F$  are supposed to be fixed at  $\widehat{X}_1$ , which makes some of such singularities occurring at  $\mathbb{S}_{\tau=1}^1$  stable under allowed isotopies.

*Step 2.* Now we are going to get rid of all local extrema of  $\theta|_{\text{int}(F) \setminus \mathbb{S}_{\tau=0}^1}$  and to make all connected components of  $\mathcal{P}_\theta \cap F$  simply connected for all  $\theta \in \mathbb{S}^1$ . To this end, we use the finger move trick introduced in a similar situation by T. Ito and K. Kawamuro in [20].

**Definition 18.** By a *finger move disc* we call a pizza slice  $\nabla = \nabla(\theta_1, \theta_2, \varphi_0, a)$  of the form  $[\theta_1, \theta_2] \times \{\varphi_0\} \times [0, a]/\sim$ , where  $\theta_1, \theta_2, \varphi_0 \in \mathbb{S}^1$ ,  $a \in (0, 1)$ , and the equivalence  $\sim$  is given by (1), such that:

- (1)  $\nabla$  is transverse to  $F$ ;
- (2) each connected component of  $\nabla \cap F$  is an arc intersecting each radial arc  $\{\theta\} \times \{\varphi_0\} \times [0, a]$ ,  $\theta \in [\theta_1, \theta_2]$ , exactly once;
- (3)  $\nabla$  is disjoint from (multiple) saddle critical points of  $\theta|_{F \setminus \mathbb{S}_{\tau=0}^1}$ ;
- (4)  $\nabla$  is disjoint from the graph  $\widehat{X_1 \cup X_2}$ ,

see examples in the left pictures of Fig. 19 and 20.

**Lemma 3.** *There exists a finite collection of pairwise disjoint finger move discs  $Y = \{\nabla_1, \dots, \nabla_m\}$  such that, for any  $\theta \in \mathbb{S}^1$ , any simple closed curve in  $F \cap \mathcal{P}_\theta$  intersects at least one of them.*

*Proof.* We start by constructing, for any  $\theta_0 \in \mathbb{S}^1$ , a family  $Y_{\theta_0}$  of pairwise disjoint finger move discs such that their union intersects any simple closed curve in  $F \cap \mathcal{P}_\theta$  if  $\theta$  is sufficiently close to  $\theta_0$ .

If  $p = (\theta_0, \varphi_0, a)$  is a local minimum of the restriction  $\theta|_{\text{int}(F) \setminus \mathbb{S}_{\tau=0}^1}$ , then for a small enough  $\varepsilon > 0$ , the disc  $\nabla(\theta_0, \theta_0 + \varepsilon, \varphi_0, a)$  will be a finger move disc that intersects all the circles in  $F \cap \mathcal{P}_\theta$ ,  $\theta \in (\theta_0, \theta_0 + \varepsilon)$ , located in a small neighborhood of  $p$ . We include it into  $Y_{\theta_0}$ .

Similarly, if  $p = (\theta_0, \varphi_0, a)$  is a local maximum of the restriction  $\theta|_{F \setminus \mathbb{S}_{\tau=0}^1}$ , then we include into  $Y_{\theta_0}$  the finger move disc  $\nabla(\theta_0 - \varepsilon, \theta_0, \varphi_0, a)$  with small enough  $\varepsilon > 0$ .

The finger moves discs we have added to  $Y_{\theta_0}$  so far are called *unmovable* (because the parameter  $\varphi_0$  is prescribed by the position of the critical point). Now we add to  $Y_{\theta_0}$  some finite number of *movable* finger move discs so that every simple closed curve in  $F \cap \mathcal{P}_\theta$  is intersected by at least one of them. The union of all discs in  $Y_{\theta_0}$  will also intersect all simple closed curves in  $F \cap \mathcal{P}_\theta$  for any  $\theta$  sufficiently close to  $\theta_0$ .

Now by the compactness of  $\mathbb{S}^1$  we can choose finitely many  $\theta_1, \dots, \theta_m \in \mathbb{S}^1$  so that the union of all finger move discs from  $Y = Y_{\theta_1} \cup \dots \cup Y_{\theta_m}$  intersect any simply closed curve contained in  $F \cap \mathcal{P}_\theta$  for any  $\theta$ . However, some of these discs may intersect each other.

Due to the restrictions we put on  $F$  at Step 1 the unmovable discs in  $Y$  are already pairwise disjoint (they occur at different  $\varphi$ 's). We can alter the parameters of the movable discs so as to make all discs from  $Y$  pairwise disjoint and still have the property that every simple closed curve in  $F \cap \mathcal{P}_\theta$  is intersected by a disc from  $Y$  for any  $\theta \in \mathbb{S}^1$ .  $\square$

Having chosen a collection  $Y$  of finger move discs as in Lemma 3 we now apply a *finger move* to  $F$  for each disc  $\nabla \in Y$ . By this we mean an isotopy in a small neighborhood of  $\nabla$  that pushes  $F$  across  $\nabla$  toward  $\mathbb{S}_{\tau=0}^1$  as shown in Fig. 19 and 20.

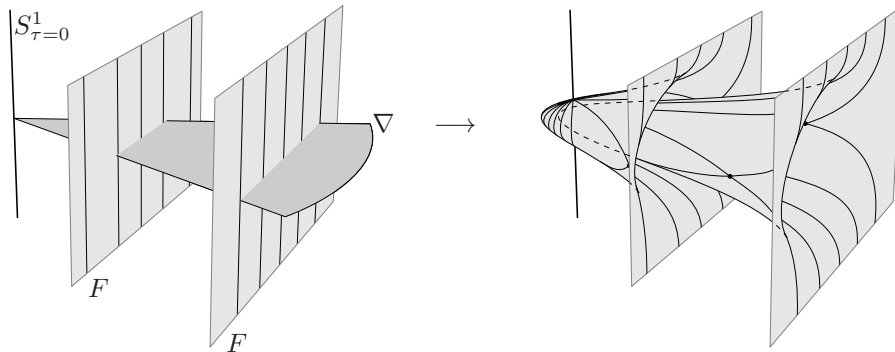


FIGURE 19. Finger move for a movable finger move disc

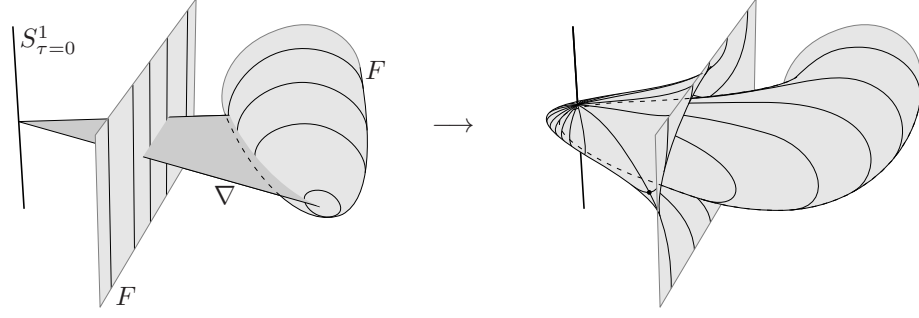


FIGURE 20. Finger move for an unmovable finger move disc

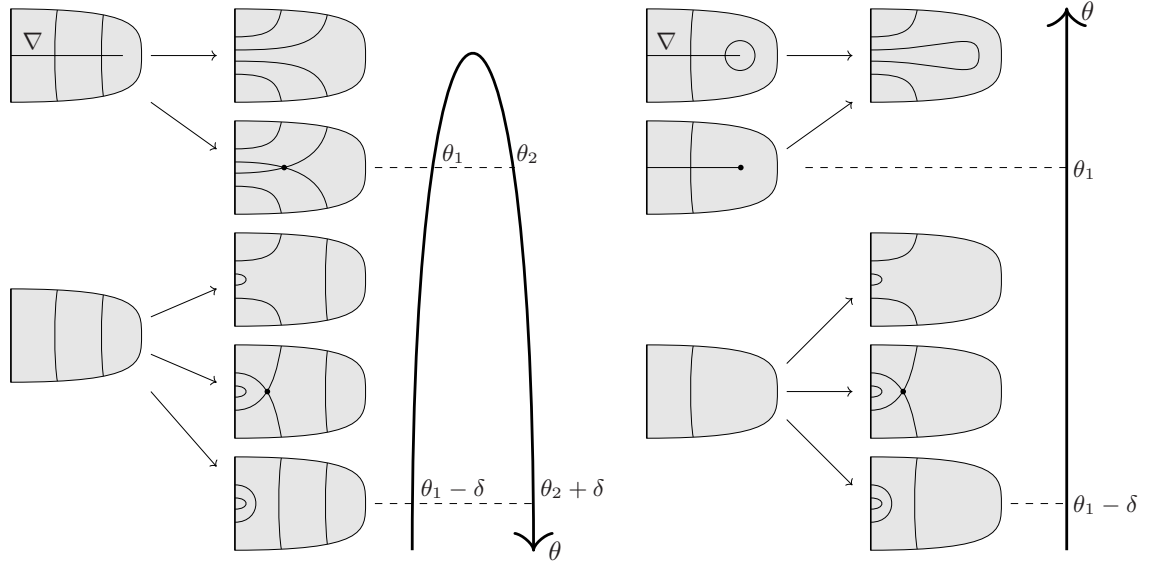


FIGURE 21. Changes in the sections  $F \cap \mathcal{P}_\theta$  occurring as a result of a finger move. Pictures on the left illustrate the movable disc case. The pictures on the right correspond to the situation when  $\theta|_{F \setminus \mathbb{S}^1_{\tau=0}}$  has a local minimum in  $\mathcal{P}_{\theta_1}$ . The small arcs created as a result of the move are preserved in  $\mathcal{P}_\theta$  for  $\theta \in [\theta_2 + \delta, \theta_1 - \delta]$ .

The intersection of  $F$  with pages  $\mathcal{P}_\theta$  is altered as indicated in Fig. 21. Since the discs in  $Y$  are disjoint, the corresponding finger moves can be done so that they do not interfere with each other.

As a result of this step we have that the intersection of  $F$  with every page  $\mathcal{P}_\theta$  is a union of pairwise disjoint arcs with endpoints on  $\mathbb{S}^1_{\tau=0}$  and possibly a star graph having a  $n$ -valent vertex,  $n > 2$ , in the interior of  $\mathcal{P}_\theta$  and 1-valent vertices at  $\mathbb{S}^1_{\tau=0}$ . There may be only finitely many pages containing such a star graph. By a small deformation of  $F$ , if necessary, we can ensure that the pages containing the star graphs do not contain edges of the graph  $\widehat{X}_2$ .

*Step 3.* At this and the next step we apply an isotopy to  $F$  such that the combinatorics of the intersection of  $F$  with each page  $\mathcal{P}_\theta$  remains unchanged. By such an isotopy we can achieve the following:

- (1)  $F$  has only finitely many intersections with  $\mathbb{S}^1_{\tau=1}$  and is orthogonal to  $\mathbb{S}^1_{\tau=1}$  at all those points;
- (2) whenever  $F \cap \mathcal{P}_\theta$  contains a star-like graph this graph must have the form  $\widehat{Q}$ , where  $Q$  is a finite subset of the meridian  $\{\theta\} \times \mathbb{S}^1$ . This means, in particular, that all critical points of  $\theta|_{F \setminus \mathbb{S}^1_{\tau=0}}$  occur at  $\mathbb{S}^1_{\tau=1}$ ;

- (3) whenever a connected component  $\beta$  of  $F \cap \mathcal{P}_\theta$  contains the center  $\mathcal{P}_\theta \cap \mathbb{S}_{\tau=1}^1$  of the page  $\mathcal{P}_\theta$ , we have that  $\beta$  is either a star graph or an arc of the form  $\widehat{v}_1 \cup \widehat{v}_2$  with  $v_1, v_2 \in \{\theta\} \times \mathbb{S}^1$ ;
- (4) for any  $\theta \in \mathbb{S}^1$ , any connected component  $\beta$  of  $F \cap \mathcal{P}_\theta$  not containing the center of the page  $\mathcal{P}_\theta$  intersects any arc of the form  $\widehat{v}$ ,  $v \in \{\theta\} \times \mathbb{S}^1$ , at most once;
- (5) every connected component of  $F$  intersects  $\mathbb{S}_{\tau=1}^1$ .

Fig. 22 demonstrates the idea of such an isotopy. First, we pull all critical points of  $\theta|_{F \setminus \mathbb{S}_{\tau=0}^1}$  to the

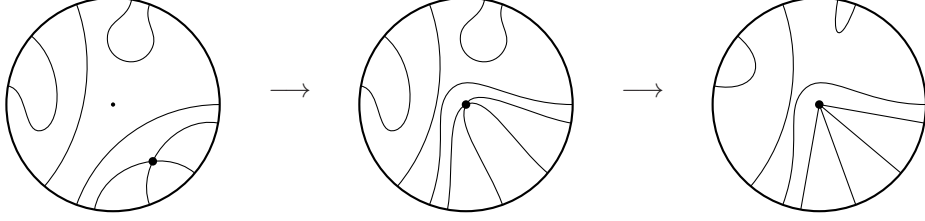


FIGURE 22. Isotopy at Step 3

circle  $\mathbb{S}_{\tau=1}^1$ . This may require to introduce more intersection points of  $F$  and  $\mathbb{S}_{\tau=1}^1$ . If there is a spherical connected component of  $F$  that does not intersect  $\mathbb{S}_{\tau=1}^1$  (non-spherical ones need not to be taken care of since they must already intersect  $\mathbb{S}_{\tau=1}^1$  by this moment) we also pull it to this circle to create an intersection. We keep fixed  $F \cap \mathbb{S}_{\tau=1}^1$  from now on.

To obtain the desired isotopy we proceed as follows. First, we make  $F$  orthogonal to  $\mathbb{S}_{\tau=1}^1$  at all the intersections and straighten the arcs joining the points from  $F \cap \mathbb{S}_{\tau=1}^1$  with  $\mathbb{S}_{\tau=0}^1$ . This may include a small deformation in the  $\theta$ -direction, in particular, to ensure that the arcs have a proper direction at  $F \cap \mathbb{S}_{\tau=1}^1$ . All the other deformations at this step can be made ‘pagewise’.

Then we pull tight all the arcs in each intersection  $F \cap \mathcal{P}_\theta$  that do not cross  $\mathbb{S}_{\tau=1}^1$  so as to ensure Condition (4) above. The fact that there is no topological obstruction to do this in all pages simultaneously follows from Smale’s theorem on contractibility of the group of diffeomorphisms of a 2-disc fixed at boundary.

We are ready to produce the sought-for diagram  $\Pi$ . For every connected component  $\beta$  of  $F \cap \mathcal{P}_\theta$  that has the form of an arc not passing through the center of the page  $\mathcal{P}_\theta$ , there are  $\varphi_1, \varphi_2 \in \mathbb{S}^1$  such that  $\beta$  intersects  $\widehat{v}$ ,  $v \in \theta \times \mathbb{S}^1$ , if and only if  $v \in \{\theta\} \times [\varphi_1, \varphi_2]$ . We will express this by saying that  $\beta$  covers the interval  $[\varphi_1, \varphi_2]$ .

If a page  $\mathcal{P}_\theta$  contains an arc covering  $[\varphi_1, \varphi_2]$ , then so does the page  $\mathcal{P}_{\theta'}$  for any  $\theta'$  close enough to  $\theta$ . Moreover, if the page  $\mathcal{P}_{\theta_1}$  contains an arc covering the interval  $[\varphi_1, \varphi_2]$  and  $\mathcal{P}_{\theta_2}$  does not do so, then there is an intersection point  $F \cap \mathbb{S}_{\tau=1}^1$  in each of the regions  $\theta \in (\theta_1, \theta_2)$  and  $\theta \in (\theta_2, \theta_1)$ .

Since there are only finitely many points in  $F \cap \mathbb{S}_{\tau=1}^1$ , for any fixed  $\varphi_1, \varphi_2 \in \mathbb{S}^1 \cap F$ ,  $\varphi_1 \neq \varphi_2$ , the set of all  $\theta$  such that the page  $\mathcal{P}_\theta$  contains an arc covering the interval  $[\varphi_1, \varphi_2]$  is a union of finitely many pairwise disjoint intervals  $(\theta'_1, \theta''_1), \dots, (\theta'_k, \theta''_k)$ ,  $k \geq 0$ . Indeed, it is an open subset of  $\mathbb{S}^1$ , but it cannot be the whole of  $\mathbb{S}^1$  as this would mean that  $F$  has a spherical component that does not intersect  $\mathbb{S}_{\tau=1}^1$ .

We then include in  $\Pi$  the rectangles  $[\theta'_i, \theta''_i] \times [\varphi_1, \varphi_2]$ ,  $i = 1, \dots, k$ , and do so for all possible choices of  $\varphi_1, \varphi_2$  (there are only finitely many of them since  $\mathbb{S}_{\tau=0}^1 \cap F$  is finite).

**Lemma 4.** *The set  $\Pi$  of rectangles obtained in this way is a rectangular digram of a surface.*

*Proof.* To see this, we first examine a neighborhood of a meridian  $\{\theta_0\} \times \mathbb{S}^1$  such that  $F$  passes through the center of the page  $\mathcal{P}_{\theta_0}$ . Such meridians are the only ones that can contain vertical sides of the rectangles from  $\Pi$ . Assume for the moment that the center  $p$  of this page is an interior point of  $F$ .

The intersection  $F \cap \mathcal{P}_{\theta_0}$  contains a singular component  $\Gamma$  that has the form  $\widehat{v}_1 \cup \widehat{v}_2 \cup \dots \cup \widehat{v}_{2k}$ , where  $k \in \mathbb{N}$ , and  $v_i = (\theta_0, \varphi_i)$ ,  $i = 1, \dots, 2k$ , are  $2k$  pairwise distinct points of the meridian  $\{\theta_0\} \times \mathbb{S}^1$ . We number them in the cyclic order they appear on the meridian so that the intervals  $(\varphi_1, \varphi_2), (\varphi_2, \varphi_3), \dots, (\varphi_{2k}, \varphi_1)$  are pairwise disjoint.

Any other component of  $F \cap \mathcal{P}_{\theta_0}$  is an arc covering a subinterval of  $(\varphi_i, \varphi_{i+1})$ ,  $i \in \{1, \dots, 2k\}$ , where we put  $\varphi_{2k+1} = \varphi_1$ . When  $\theta$  deviates from  $\theta = \theta_0$  the singular component  $\Gamma$  gets resolved into a family of arcs. When it deviates one way (say,  $\theta < \theta_0$ )  $\Gamma$  resolves to arcs covering all the intervals  $[\varphi_i, \varphi_{i+1}]$  with odd  $i$ 's, and when  $\theta$  deviates the other way  $\Gamma$  resolves to such arcs with even  $i$ 's.

Thus, the rectangles from  $\Pi$  that have a vertical side on  $\{\theta_0\} \times \mathbb{S}^1$  will be arranged near this meridian in a checkerboard manner, see the left picture in Fig. 23. Note that all other rectangles intersecting the

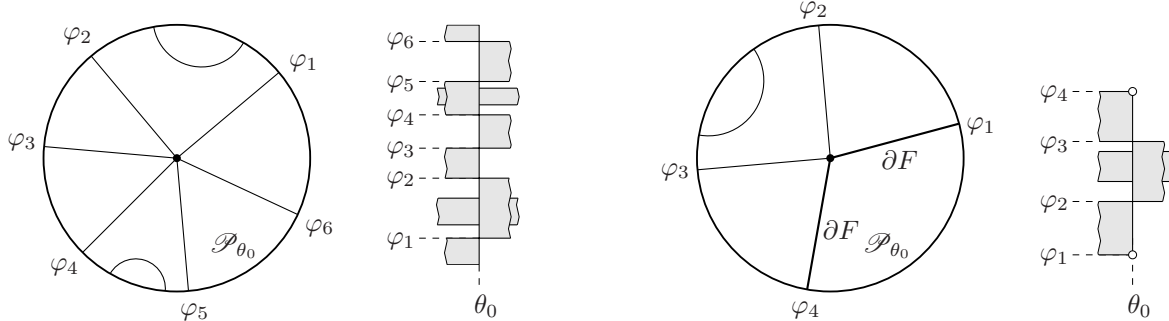


FIGURE 23. The rectangles from  $\Pi$  near a ‘critical’ meridian

meridian  $\{\theta_0\} \times \mathbb{S}^1$  will be disjoint from the longitudes  $\mathbb{S}^1 \times \{\varphi_i\}$ ,  $i = 1, \dots, 2k$ . In other words, vertices of rectangles cannot lie in the interior of other rectangles.

If  $p$  lies at the boundary  $\partial F$ , we will have a similar picture with the only difference that the vertical sides of the rectangles now cover not the whole meridian  $\{\theta_0\} \times \mathbb{S}^1$  but a proper subarc, see the right picture in Fig. 23.

One can now see that any two rectangles in  $\Pi$  are compatible. Indeed, let  $r_1 = [\theta'_1, \theta''_1] \times [\varphi'_1, \varphi''_1]$  and  $r_2 = [\theta'_2, \theta''_2] \times [\varphi'_2, \varphi''_2]$  be two rectangles from  $\Pi$ . Suppose that their interiors have a non-empty intersection. This means that  $(\theta'_1, \theta''_1) \cap (\theta'_2, \theta''_2) \neq \emptyset$  and  $(\varphi'_1, \varphi''_1) \cap (\varphi'_2, \varphi''_2) \neq \emptyset$ . For any  $\theta \in (\theta'_1, \theta''_1) \cap (\theta'_2, \theta''_2)$  there are two disjoint arcs in  $F \cap \mathcal{P}_\theta$  one of which covers  $[\varphi'_1, \varphi''_1]$  and the other  $[\varphi'_2, \varphi''_2]$ . This is possible only if these intervals are disjoint or one is contained in the other. The former case does not occur as the intervals have non-empty intersection.

Thus, without loss of generality, we may assume  $[\varphi'_1, \varphi''_1] \subset (\varphi'_2, \varphi''_2)$ . The meridians  $\{\theta'_1\} \times \mathbb{S}^1$  and  $\{\theta''_1\} \times \mathbb{S}^1$  contain the vertical sides of  $r_1$ . As the reasoning above shows, there can be no arc covering  $[\varphi'_2, \varphi''_2]$  in  $F \cap \mathcal{P}_\theta$  if  $\theta$  is close enough to  $\theta'_1$  or  $\theta''_1$ , since otherwise a vertex of  $r_1$  would lie in the interior of  $r_2$ . This means  $\theta'_1, \theta''_1 \notin [\theta'_2, \theta''_2]$ , which implies  $[\theta'_2, \theta''_2] \subset (\theta'_1, \theta''_1)$ . Therefore,  $r_1$  and  $r_2$  are compatible.

It also follows from the above arguments that two rectangles from  $\Pi$  cannot share a nontrivial subarc of their vertical sides. Neither they can share a nontrivial subarc of horizontal sides as this would imply a singularity of  $F$  at  $\mathbb{S}^1_{\tau=0}$  that is not allowed for surfaces with corners.

Thus, if the interiors of two rectangles from  $\Pi$  are disjoint, then the intersection of these rectangles will be a subset of their vertices. So, any two rectangles from  $\Pi$  are compatible.

The free vertices of  $\Pi$  are by construction such  $v \in \mathbb{T}^2$  that  $\widehat{v} \subset \partial F$ . There can be at most two on each meridian or longitude as the converse would imply that  $\partial F$  is a graph having vertices of valence greater than two.  $\square$

*Step 4.* We now have that the intersection of surfaces  $F$  and  $\widehat{\Pi}$  with every page have the same combinatorial structure. This means that, for every arc not passing through the center of the page, in each of this intersections, there is an arc in the other one covering the same interval. Whenever one of the intersections contains a singular component (i.e. a star graph or an arc passing through the center of the page) the other intersection contains exactly the same one.

An isotopy from  $F$  to  $\widehat{\Pi}$  is now obvious. For every  $v \in \mathbb{T}^2$  either  $\widehat{v}$  is contained in both  $F$  and  $\widehat{\Pi}$  or the sets  $\widehat{v} \cap F$  and  $\widehat{v} \cap \widehat{\Pi}$  are finite and have the same number of points. In the latter case we simply move the points from  $F \cap \widehat{v}$  to the corresponding points of  $\widehat{\Pi} \cap \widehat{v}$  along  $\widehat{v}$ .

This concludes the proof of Proposition 5.  $\square$

## 3. LEGENDRIAN LINKS AND LEGENDRIAN GRAPHS

**3.1. Definitions. Equivalence of Legendrian graphs.** First, recall some basic things from contact topology.

The plane field  $\xi_+$  defined by (4) is one of many possible presentations of *the standard contact structure on  $\mathbb{S}^3$* . For any  $p \in \mathbb{S}^3$  the plane  $\xi_+(p)$  is called *the contact plane at  $p$* . Diffeomorphisms  $\mathbb{S}^3 \rightarrow \mathbb{S}^3$  preserving this plane field are called *contactomorphisms*.

The contact structure  $\xi_+$  comes with a *coorientation*, which is defined by demanding that the 1-form  $\alpha_+ = \cos^2(\pi\tau/2)d\varphi + \sin^2(\pi\tau/2)d\theta$ , which defines  $\xi_+$ , evaluates positively on a positively oriented transverse vectors. The standard (cooriented) contact structure is defined also by any positive multiple  $\alpha = f\alpha_+$  of  $\alpha_+$ ,  $f : \mathbb{S}^3 \rightarrow (0, \infty)$ ,  $f \in C^\infty$ . Any such form  $\alpha$  will be referred to as *a standard contact form*. It has the property that  $\alpha \wedge d\alpha$  is a positive multiple of the standard volume element of  $\mathbb{S}^3$  at every point. By Darboux's theorem all contact structures are locally equivalent.

**Definition 19.** A cusp-free piecewise smooth curve  $\gamma$  in  $\mathbb{S}^3$  is called *Legendrian* if it is composed of  $C^1$ -smooth arcs tangent to the contact plane  $\xi_+(p)$  at every point  $p \in \gamma$ .

A *Legendrian link* is a link in  $\mathbb{S}^3$  each component of which is a Legendrian curve.

A *Legendrian graph* is a compact 1-dimensional CW-complex  $\Gamma$  embedded in  $\mathbb{S}^3$  such that every embedded curve in  $\Gamma$  is Legendrian (in particular, any such curve must be cusp-free).

In this paper we understand graphs as topological subspaces in  $\mathbb{S}^3$ , so, we do not distinguish between two graphs if one is obtained from the other by subdividing an edge by new vertices.

For an oriented Legendrian link  $L$  one defines *the Thurston–Bennequin number  $\text{tb}_+(L)$  of  $L$*  as  $\text{lk}(L, L')$ , where the link  $L'$  is obtained from  $L$  by a small shift in a direction transverse to  $\xi_+$ . This is known to be a Legendrian link invariant. For a link of the form  $L = \widehat{R}$ , where  $R$  is a rectangular diagram of a link,  $\text{tb}_+(L)$  coincides with  $\text{tb}_+(R)$ , see Definition 16 and Proposition 4. If  $L$  is a Legendrian sublink of  $\partial F$ , where  $F$  is a surface, one also defines *the Thurston–Bennequin number of  $L$  relative to  $F$* :

$$\text{tb}_+(L; F) = \text{tb}_+(L) - \text{lk}(L, L^F),$$

which agrees with Definition 17 given in the ‘rectangular’ terms.

**Definition 20.** Let  $\Gamma_1, \Gamma_2$  be two Legendrian graphs and  $p \in \Gamma_1 \cap \Gamma_2$  a point. We say that  $\Gamma_1$  and  $\Gamma_2$  are obtained from each other by *an angle adjustment at  $p$*  if there is a local coordinate system  $x, y, z$  near  $p$  and an  $\varepsilon > 0$  such that

- (1)  $p$  is the origin of the system  $x, y, z$ ;
- (2)  $dz + x dy - y dx$  is a standard contact form near  $p$ ;
- (3)  $\Gamma_1$  and  $\Gamma_2$  coincide outside of the neighborhood  $U$  of  $p$  that is defined by  $x^2 + y^2 < \varepsilon$ ,  $|z| < \varepsilon$ , and in a small tubular neighborhood of  $\partial U$ ;
- (4) for each  $i = 1, 2$ , the closure of the intersection  $\Gamma_i \cap U$  is a simple arc containing  $p$  and having endpoints at the cylinder  $C = \{(x, y, z) ; x^2 + y^2 = \varepsilon\}$ , or a star graph whose internal node is  $p$  and whose one-valent vertices lie in  $C$ ;
- (5) for each  $i = 1, 2$ , the projection of  $\Gamma_i \cap U$  to the  $xy$ -plane (which is the contact plane at  $p$ ) along the  $z$ -direction is injective;
- (6) for each  $i = 1, 2$  the closure of each connected component of  $(\Gamma_i \cap U) \setminus \{p\}$  is a smooth arc.

If  $\Gamma'_2$  and  $\Gamma''_2$  are two Legendrian graphs each of which is obtained from  $\Gamma_1$  by an angle adjustment at a vertex  $p \in \Gamma_1$  of valence  $> 1$  and the edges of  $\Gamma'_2$  emanating from  $p$  have the same tangent rays as the respective edges of  $\Gamma''_2$  we say that *the angle adjustments  $\Gamma_1 \mapsto \Gamma'_2$  and  $\Gamma_1 \mapsto \Gamma''_2$  are equivalent*.

**Proposition 6.** (i) *Let  $\Gamma$  be a Legendrian graph and  $p \in \Gamma$  its vertex of valence  $k > 1$ . Let  $r_1, \dots, r_k$  be the tangent rays to the edges of  $\Gamma$  at  $p$ . Let  $r'_1, \dots, r'_k$  be another family of pairwise distinct rays emanating from  $p$  and lying in the contact plane  $\xi_+(p)$ . Assume that  $r'_1, \dots, r'_k$  follow in this plane in the same circular order as  $r_1, \dots, r_k$  do.*

*Then for any neighborhood  $U$  of  $p$  there exists an angle adjustment  $\Gamma \mapsto \Gamma'$  such that  $\Gamma \setminus U = \Gamma' \setminus U$  and if an edge of  $\Gamma$  is tangent to  $r_i$  at  $p$ , then the respective edge of  $\Gamma'$  is tangent to  $r'_i$ .*



(ii) Let Legendrian graphs  $\Gamma'$  and  $\Gamma''$  be obtained from a Legendrian graph  $\Gamma$  by equivalent angle adjustments. Then there exists a contactomorphism  $\psi : \mathbb{S}^3 \rightarrow \mathbb{S}^3$  such that  $\psi(\Gamma') = \Gamma''$ .

*Proof.* (i) Let  $x, y, z$  be a local coordinate system as in Definition 20. A Legendrian arc is uniquely recovered from its projection to the  $xy$ -plane plus the knowledge of the  $z$ -coordinate of a single point, since along the arc we have  $dz = -x dy + y dx$ .

Let  $V \subset U$  be a small cylindrical neighborhood of  $p$  such that  $\Gamma \cap V$  is projected to the  $xy$ -plane injectively and the closure of the projection has the form  $\gamma_1 \cup \dots \cup \gamma_k$ , where  $\gamma_i$  is a smooth arc connecting  $p$  with a point at  $\partial V \cap \{z = 0\}$  and tangent to  $r_i$  at  $p$ ,  $i = 1, \dots, k$ .

We can obviously find another family of arcs  $\gamma'_1, \dots, \gamma'_k$  that also form a star graph in  $V \cap \{z = 0\}$  such that for any  $i = 1, \dots, k$  the following hold:

- (1)  $\partial\gamma_i = \partial\gamma'_i$ ;
- (2)  $\gamma'_i$  is tangent to  $r'_i$  at  $p$  and to  $\gamma_i$  at the other endpoint;
- (3)  $\int_{\gamma_i} (x dy - y dx) = \int_{\gamma'_i} (x dy - y dx)$  if  $\gamma_i$  and  $\gamma'_i$  are oriented coherently.

Now  $\Gamma'$  is uniquely defined by demanding that  $\Gamma' \setminus U = \Gamma \setminus U$  and that the projection to the  $xy$ -plane of  $\Gamma' \cap V$  is  $\gamma'_1 \cup \dots \cup \gamma'_k$ .

(ii) Let  $\gamma'_1, \dots, \gamma'_k$  be as above and  $\gamma''_1, \dots, \gamma''_k$  be another family of arcs with the same properties. One can see that there is an isotopy from one family to the other such that the tangent rays at the endpoints to each arc as well as the integral of the form  $x dy - y dx$  along each arc stay fixed, and the interiors of arcs remain disjoint. This means that there is a smooth isotopy from  $\Gamma'$  to  $\Gamma''$  (the latter obtained similarly to  $\Gamma'$  by using arcs  $\gamma''_i$  in place of  $\gamma'_i$ ) in the class of Legendrian graphs such that the tangent rays to the edges of the graph at  $p$  and the intersection of the graph with the exterior of  $V$  remain fixed during the isotopy. By smoothness of this isotopy we mean that it changes only a part of a graph consisting of smooth arcs, and its restriction to these arcs is smooth.

It is then classical to see that such an isotopy can be realized by an ambient isotopy in the class of contactomorphisms, see [15, Theorem 2.6.2].  $\square$

*Remark 5.* The integral of the form  $x dy - y dx$  over a closed curve in the  $xy$ -plane is twice the oriented area bounded by the curve. So, if we want to make an angle adjustment that rotates a portion of an edge around an endpoint  $p$ , then some farther portion must rotate in the opposite direction, see Fig. 24.

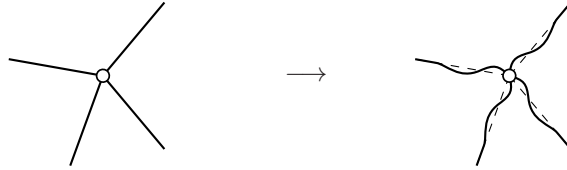


FIGURE 24. Angle adjustment

**Proposition 7.** Let  $\Gamma_0$  and  $\Gamma_1$  be two Legendrian graphs. The following two conditions are equivalent:

- (1)  $\Gamma_1$  can be obtained from  $\Gamma_0$  by an angle adjustment followed by a contactomorphism of  $\mathbb{S}^3$ ;
- (2) there exists an isotopy  $\eta : [0, 1] \times \Gamma_0 \rightarrow \mathbb{S}^3$  and a finite collection of regularly parametrized closed arcs  $\gamma_1, \dots, \gamma_k \subset \Gamma_0$  such that
  - (a) the arcs  $\gamma_i$ ,  $i = 1, \dots, k$ , cover the whole of  $\Gamma_0$ ;
  - (b)  $\eta_t(\Gamma_0)$  is a Legendrian graph for any  $t \in [0, 1]$ ;
  - (c)  $\eta_0 = \text{id}_{\Gamma_0}$  and  $\eta_1(\Gamma_0) = \Gamma_1$ ;
  - (d)  $\{\eta_t(\gamma_i) ; t \in [0, 1]\}$  is a  $C^1$ -continuous family of regularly parametrized arcs for each  $i = 1, \dots, k$ .

We skip the elementary but boring proof.

**Definition 21.** If the two equivalent conditions from Proposition 7 hold we say that *the Legendrian graphs  $\Gamma_0$  and  $\Gamma_1$  are equivalent*. If, in addition, an isotopy  $\eta$  from  $\Gamma_0$  to  $\Gamma_1$  satisfying Condition (2) from Proposition 7 exists such that  $\eta$  is fixed on a subset  $X \subset \mathbb{S}^3$  we say that  *$\Gamma_0$  and  $\Gamma_1$  are equivalent relative to  $X$* .

*Remark 6.* Condition (2) from Proposition 7 has the same meaning as the definition of the Legendrian graph equivalence given in [27]. Our angle adjustment operation is a generalization of the notion of a canonical smoothing defined in [8, 9], which can be considered as an angle adjustment applied to a Legendrian link so that the result is a smooth Legendrian link. As noted in [27] the results of two different canonical smoothings are related by a contactomorphism, so extending the class of Legendrian links from smooth to cusp-free piecewise smooth neither creates any new class of Legendrian links nor merges any two distinct classes together.

### 3.2. Rectangular diagrams of graphs.

**Definition 22.** A *rectangular diagram of a graph* is a triple  $G = (\Theta, \Phi, E)$ , where  $\Theta$  and  $\Phi$  are finite subsets of  $\mathbb{S}^1$  and  $E$  is a subset of  $\Theta \times \Phi \subset \mathbb{T}^2$ .

We interpret  $\Theta$  as a subset of  $\mathbb{S}_{\tau=1}^1 \subset \mathbb{S}^3$  and  $\Phi$  as a subset of  $\mathbb{S}_{\tau=0}^1$ . The graph associated with  $G$  is the following union:

$$\widehat{G} = \Theta \cup \Phi \cup \left( \bigcup_{v \in E} \widehat{v} \right) \subset \mathbb{S}^3.$$

Unless we want to deal with graphs that have isolated vertices we can forget about  $\Theta$  and  $\Phi$  in this definition and understand a rectangular diagram of a graph simply as a finite subset of  $\mathbb{T}^2$ . Indeed, if  $\widehat{G}$  does not have isolated vertices, then  $\Theta$  and  $\Phi$  can be recovered from  $E$ , since they are just the projections of  $E \subset \mathbb{S}^1 \times \mathbb{S}^1$  to the  $\mathbb{S}^1$ 's. In this paper graphs with isolated vertices are not needed, but we prefer to give the general definition for future reference.

In the sequel, for simplicity, we assume all considered graphs not to have isolated vertices, so ‘a rectangular diagram of a graph’ will mean just a finite subset of the torus  $\mathbb{T}^2$ . The following result obviously remains true if isolated vertices are allowed.

Note that all graphs of the form  $\widehat{G}$ , where  $G$  is a rectangular diagram of a graph, are Legendrian graphs. They also remain Legendrian if  $\xi_+$  is replaced by  $\xi_-$  in the definition.

**Proposition 8.** Let  $G$  be a rectangular diagram of a graph and  $\Gamma$  a Legendrian graph such that  $\Gamma \cap \widehat{G} \subset \mathbb{S}_{\tau=0}^1 \cup \mathbb{S}_{\tau=1}^1$  and  $\Gamma \cup \widehat{G}$  is also a Legendrian graph. Then there exists a rectangular diagram of a graph  $G'$  such that the Legendrian graphs  $\widehat{G}'$  and  $\Gamma$  are equivalent relative to  $\widehat{G}$ .

*Proof.* The only thing we need is to extend the Approximation Principle to Legendrian graphs. To this end, we look more closely at the torus projections of Legendrian links, which are similar in nature to widely explored front projections.

Indeed, let  $\gamma$  be a Legendrian curve disjoint from  $\mathbb{S}_{\tau=0}^1$  and  $\mathbb{S}_{\tau=1}^1$ . Its torus projection locally is a cusped curve, and  $\gamma$  can be recovered from the torus projection since the  $\tau$  coordinate is determined by the slope  $d\varphi/d\theta$ :

$$\tau = \frac{2}{\pi} \arctan \sqrt{-d\varphi/d\theta}.$$

The slope of the torus projection is everywhere negative and continuous, and the larger the absolute value of the slope the ‘higher’ is the corresponding point of the curve. The slope tends to  $\infty$  when  $\gamma$  approaches  $\mathbb{S}_{\tau=1}^1$  and to 0 when  $\gamma$  approaches  $\mathbb{S}_{\tau=0}^1$ .

Thus, a Legendrian curve disjoint from  $\mathbb{S}_{\tau=0}^1$  and  $\mathbb{S}_{\tau=1}^1$  can be recovered from its torus projection, and an isotopy in the class of Legendrian curves can be described in terms of the projection.

Now we show how to produce  $G'$ . First, we apply an isotopy that will move all vertices of  $\Gamma$  to  $\mathbb{S}_{\tau=0}^1 \cup \mathbb{S}_{\tau=1}^1$  (this can be realized by a contactomorphism of  $\mathbb{S}^3$  due to [15, Theorem 2.6.2]) and make the rest of  $\Gamma$  have only finitely many points of tangency with arcs of the form  $\widehat{v}$ ,  $v \in \mathbb{T}^2$ . Such tangencies outside of the circles  $\mathbb{S}_{\tau=0,1}^1$  are responsible for cusps of the torus projection.



Now the torus projection of every edge of  $\Gamma$  is a cusped open arc (in general, with self-intersections) that approaches two distinct points at the ends, and at each of these points have either vertical or horizontal slope. Cusps divide this arc into finitely many subarcs of negative slope.

We approximate each of these subarcs by a staircase arc so that (see Fig. 25):

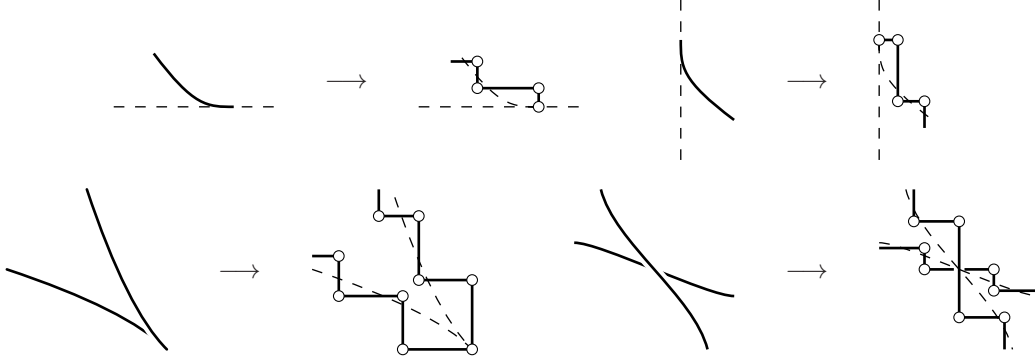


FIGURE 25. Approximating the torus projection of a Legendrian graph by staircases

- (1) there is an isotopy from the subarc to the corresponding staircase in  $\mathbb{T}^2 \setminus G$ ;
- (2) intersections of the staircases occur exactly at intersections of the corresponding subarcs;
- (3) the endpoints of the staircase arcs are the same as those of the approximated subarcs;
- (4) if the subarc has vertical (respectively, horizontal) slope at an endpoint, then the staircase approximation has horizontal (respectively, vertical) one;
- (5) at every cusp of the torus projection the corresponding staircases arrive vertically, and the other horizontally;
- (6) no two edges in the staircases occur at the same meridian or longitude, and no edge occurs on a meridian or longitude already occupied by a vertex of  $G$ .

If the approximation is fine enough, then the set of all endpoints of the edges of the obtained staircases works for  $G'$ . We leave the easy details to the reader.  $\square$

#### 4. GIROUX'S CONVEX SURFACES

**4.1. Definition.** Giroux's original definition is given for closed  $C^\infty$ -smooth orientable surfaces. For surfaces with boundary it is naturally generalized for two closely related cases: surfaces with Legendrian boundary [18] and surfaces with transverse boundary [12]. We will be dealing only with surfaces with Legendrian boundary.

In order to adapt the language of rectangular diagrams to convex surfaces we need to extend the class of considered surfaces to surfaces with corners. In particular, we downgrade their smoothness class to  $C^1$ , which will be crucial at some point. Many structural results about convex surfaces remain true and require no or very little modification of the proof.

Another feature here is that we generalize Giroux's convexity to non-orientable surfaces. This generalization is quite obvious and straightforward, and many known facts about convex surfaces can be generalized accordingly at no effort.

However, we will exploit the fact that the standard contact structure of  $\mathbb{S}^3$  is coorientable.

We define convex surfaces only with respect to the standard contact structure on  $\mathbb{S}^3$ . The definition can be obviously extended to an arbitrary contact 3-manifold.

**Definition 23.** A vector field in an open subset  $U$  of  $\mathbb{S}^3$  is called *contact* if it generates a flow in  $U$  that preserves the standard contact structure.

A line element field (i.e. a smooth assignment of an unordered pair of opposite tangent vectors to each point) in  $U \subset \mathbb{S}^3$  is called *contact* if its restriction to every simply connected open subset  $V$  of  $U$  has the form  $\{u, -u\}$ , where  $u$  is a contact vector field on  $V$ .

**Definition 24.** A surface with corners  $F$  is called *convex (with respect to the standard contact structure)* if  $\partial F$  is a Legendrian link and there exists an open neighborhood  $U$  of  $F$  and a contact line element field in  $U$  transverse to  $F$ .

Note that to be convex in this sense is a global property. Locally every surface is convex.

**Definition 25.** Let  $F_0$  and  $F_1$  be two convex surfaces with corners. We say that they are *equivalent* if there exists a  $C^0$ -isotopy  $\eta : [0, 1] \times F_0 \rightarrow \mathbb{S}^3$  and finitely many points  $p_1, \dots, p_k \in \partial F_0$  such that

- (1) for every  $t \in [0, 1]$  the image  $\eta_t(F_0)$  is a convex surface with corners;
- (2)  $\eta_0 = \text{id}|_{F_0}$ ,  $\eta_1(F_0) = F_1$ ;
- (3) the restriction of  $\eta$  to  $[0, 1] \times (F_0 \setminus \{p_1, \dots, p_k\})$  is of smoothness class  $C^1$ ;
- (4) the tangent plane to  $\eta_t(F_0)$  at  $\eta_t(p)$  depends continuously on  $(t, p) \in [0, 1] \times F_0$ .

The following two statements are given for completeness of the exposition and are not used in the sequel. We skip their proofs, which are easy.

**Proposition 9.** Let  $F$  be a convex surface with corners,  $p_1, \dots, p_k$  be all the singularities of  $\partial F$ . Then for any  $\varepsilon > 0$  there exists a convex surface with corners  $F'$  equivalent to  $F$  such that  $F'$  coincides with  $F$  outside of the union of the  $\varepsilon$ -neighborhoods of  $p_1, \dots, p_k$ , and  $\partial F'$  is obtained from  $\partial F$  by a canonical smoothing.

**Proposition 10.** Let  $F_0$  and  $F_1$  be convex surfaces with smooth boundaries. Then they are equivalent if and only if there exists a smooth isotopy between them within the class of convex surfaces.

**4.2. ‘Rectangular’ surfaces are convex.** Here is the main result of this paper.

**Theorem 2.** (i) For every rectangular diagram of a surface  $\Pi$  the associated surface  $\hat{\Pi}$  is convex with respect to  $\xi_+$  (and, by symmetry, with respect to  $\xi_-$ ). For any connected component  $S$  of  $\partial \Pi$  we have

$$(7) \quad |S| \geq -2 \text{tb}_+(\hat{S}; \hat{\Pi}).$$

(ii) Let  $R$  be a rectangular diagram of a link,  $L$  a Legendrian link in  $\mathbb{S}^3$  equivalent to  $\hat{R}$ , and  $F$  a convex surface with corners such that  $L \cap F$  is a sublink of  $\partial F$ . Suppose that for any connected component  $K$  of  $L \cap F$  and the respective component  $S$  of  $R$  we have  $|S| \geq -2 \text{tb}_+(K; F)$ .

Then there exists a rectangular diagram of a surface  $\Pi$  and an isotopy taking the pair  $(L, F)$  to  $(\hat{R}, \hat{\Pi})$  and realizing an equivalence of the convex surfaces  $F$  and  $\hat{\Pi}$  in the sense of Definition 25.

*Remark 7.* The assertion of the theorem can be strengthened by requiring that the isotopy from  $(L, F)$  to  $(\hat{R}, \hat{\Pi})$  extend a prescribed isotopy from  $L$  to  $\hat{R}$  satisfying Condition (2) from Proposition 7. The proof of this requires essentially no new idea but some more technical details, which we prefer not to overload the paper by.

*Proof of part (i) of Theorem 2.* A contact line element field transverse to  $\hat{\Pi}$  can be constructed almost explicitly. Let  $r = [\theta_1, \theta_2] \times [\varphi_1, \varphi_2]$  be a rectangle from  $\Pi$ . Pick a small  $\varepsilon > 0$  and take arbitrary two  $C^\infty$ -functions  $a : [\theta_1 - \varepsilon, \theta_2 + \varepsilon] \rightarrow [-1, 1]$ ,  $b : [\varphi_1 - \varepsilon, \varphi_2 + \varepsilon] \rightarrow [-1, 1]$  such that:

- (1)  $a(\theta) = 1$  if  $\theta \in [\theta_1 - \varepsilon, \theta_1 + \varepsilon]$ ,  $b(\varphi) = -1$  if  $\varphi \in [\varphi_1 - \varepsilon, \varphi_1 + \varepsilon]$ ;
- (2)  $a(\theta) = -a(\theta_1 + \theta_2 - \theta)$  for all  $\theta$ ,  $b(\varphi) = -b(\varphi_1 + \varphi_2 - \varphi)$  for all  $\varphi$ ;
- (3)  $a'(\theta) < 0$  if  $\theta \in (\theta_1 + \varepsilon, \theta_2 - \varepsilon)$ ;  $b'(\varphi) > 0$  if  $\varphi \in (\varphi_1 + \varepsilon, \varphi_2 - \varepsilon)$ .

Such functions obviously exist. The following line element field defined in the domain

$$W_r = [\theta_1 - \varepsilon, \theta_2 + \varepsilon] * [\varphi_1 - \varepsilon, \varphi_2 + \varepsilon] \subset \mathbb{S}^1 * \mathbb{S}^1 = \mathbb{S}^3$$

is then contact:

$$(8) \quad l_r = \pm \left( a(\theta) \partial_\theta + b(\varphi) \partial_\varphi + \frac{\sin \pi \tau}{2\pi} (b'(\varphi) - a'(\theta)) \partial_\tau \right),$$

which is verified by a direct check. One can also see that it is transverse to the tile  $\hat{r}$ . Indeed, all three summands in the right hand side define vector fields that point at the same side of  $\hat{r}$  unless they vanish. (This is because the function  $h_r$  used in the definition of  $\hat{r}$  is concave in  $\theta$ , convex in  $\varphi$ , and symmetric

in the center of the rectangle.) The first summand vanishes only at the line  $\theta = (\theta_1 + \theta_2)/2$ , the second at the line  $\varphi = (\varphi_1 + \varphi_2)/2$ , so, their sum vanishes only at the center of  $r$ , where the third summand doesn't.

If  $r$  and  $r'$  are two rectangles in  $\Pi$  sharing a vertex  $v$ , and  $p$  is an interior point of  $\widehat{v}$ , then in a small neighborhood of  $p$  the line element fields  $l_r$  and  $l_{r'}$  coincide and have the form either  $\pm(\partial_\theta + \partial_\varphi)$  or  $\pm(\partial_\theta - \partial_\varphi)$ . One can also see that for any  $r \in \Pi$  the restriction of  $l_r$  on  $\mathbb{S}_{\tau=0}^1$  coincides with  $\pm\partial_\varphi$  (where defined) and on  $\mathbb{S}_{\tau=1}^1$  with  $\pm\partial_\theta$ , and that the line element field  $l_r$  is continuous where defined.

For each  $r \in \Pi$ , denote by  $V_r$  the intersection of  $W_r$  with the  $\varepsilon$ -neighborhood of  $\widehat{r}$ . If  $\varepsilon$  is chosen small enough then the interiors of  $V_r$  and  $V_{r'}$  have a non-empty intersection only if  $r$  and  $r'$  share a vertex (or two vertices, or four vertices), and then  $l_r = l_{r'}$  in  $V_r \cap V_{r'}$ .

Denote by  $l$  the line element field in  $V = \bigcup_{r \in \Pi} V_r$  whose restriction on  $V_r$  coincides with  $l_r$ . We are almost done, but there are two minor problems with  $l$ . First,  $V$  does not contain an open neighborhood of  $\widehat{\Pi}$  if  $\partial\widehat{\Pi} \neq \emptyset$ . Namely, the intersection  $\partial\widehat{\Pi} \cap (\mathbb{S}_{\tau=0}^1 \cup \mathbb{S}_{\tau=1}^1)$  does not lie in the interior of  $V$ . This can be easily resolved by adding more rectangles to  $\Pi$  so as to obtain a new diagram  $\Pi'$  such that  $\partial\widehat{\Pi}$  is contained in the interior of  $\widehat{\Pi'}$ . If we now construct  $V$  using  $\Pi'$  instead of  $\Pi$ , then the whole of  $\widehat{\Pi}$  will be contained in the interior of  $V$ .

The other problem is that  $l$  is only  $C^0$  at  $V \cap (\mathbb{S}_{\tau=0}^1 \cup \mathbb{S}_{\tau=1}^1)$ . (Everywhere else in  $V$  it is  $C^\infty$ .) This issue can be resolved as follows.

In general, if  $\alpha$  is a standard contact form, then any contact field  $X$  is recovered uniquely from the function  $f = \alpha(X)$ , which can be an arbitrary smooth function. This is done by solving at every point the following non-degenerate linear system in  $(X, c)$ , where  $c$  is an additional variable function:

$$(9) \quad \alpha(X) = f, \quad d\alpha(X, \cdot) + df + c\alpha = 0.$$

If  $f$  is varied slightly in the  $C^1$ -topology, then the corresponding  $X$  is varied slightly in  $C^0$ .

Now the point is that the evaluation of the 1-form in the right hand side of (4) on the line element field (8) gives a  $C^1$ -smooth (two-valued) function. We can approximate it by a  $C^\infty$  function making a  $C^1$ -small perturbation. This will give a  $C^\infty$  line element field  $C^0$ -close to  $l$ , which is enough to ensure that the perturbed field is still transverse to  $\widehat{\Pi}$ .

Inequality (7) follows from Proposition 4. □

To prove part (ii) of Theorem 2 we need some more preparatory work.

**4.3. Characteristic foliation.** As shown in [13] in order to see that a surface is convex in Giroux's sense it is enough to know the characteristic foliation of the surface, which we define below, and it is easier to examine this foliation than to seek for a transverse contact line element field.

**Definition 26.** Let  $F$  be a surface with corners. The *characteristic foliation* of  $F$  is the singular foliation defined by the line field  $T_p F \cap \xi_+(p)$ , where  $T_p F$  denotes the tangent plane to  $F$  at  $p$ . This foliation will be denoted by  $\mathcal{F}(F)$ . We endow it with the coorientation that is inherited from the coorientation of  $\xi_+$ .

The foliation  $\mathcal{F}(F)$  will be called *nice* if it has only finitely many singularities, i.e. points where  $F$  is tangent to  $\xi_+$ , and each of them is either an elliptic singularity (also called a *node*) near which the foliation is radial, or a (simple) saddle. Additionally, we require that if  $p$  is a singularity of  $\partial F$ , then it is a node of  $\mathcal{F}(F)$ .

The foliation  $\mathcal{F}(F)$  will be called *very nice* if it is nice and has neither a closed leaf nor a cooriented saddle connection cycle.

**Proposition 11.** *Let  $F$  be a convex surface with corners. Then there exist convex surfaces with corners  $F'$  and  $F''$  equivalent to  $F$  such that  $\partial F' = \partial F'' = \partial F$ , the foliations  $\mathcal{F}(F')$  and  $\mathcal{F}(F'')$  are nice and very nice, respectively, and, moreover, the surface  $F'$  can be chosen arbitrarily  $C^1$ -close to  $F$ . The surface  $F''$  can be chosen  $C^0$ -close to  $F$ .*

*Proof.* These facts are classical for  $C^\infty$  surfaces [13]. For completeness of the exposition we provide here a proof with some details omitted.

By a  $C^1$ -small perturbation of  $F$ , which can be made within the class of convex surfaces, we can make the set of points where  $F$  is tangent to  $\xi_+$ , which will be the singularities of  $\mathcal{F}(F)$ , finite.

We can also make the singularities of  $\mathcal{F}(F)$  be of ‘Morse type’, i.e. nodes and saddles. However, nodes require a little more care as typically the foliation is not radial around them, see Fig. 26. It can be made

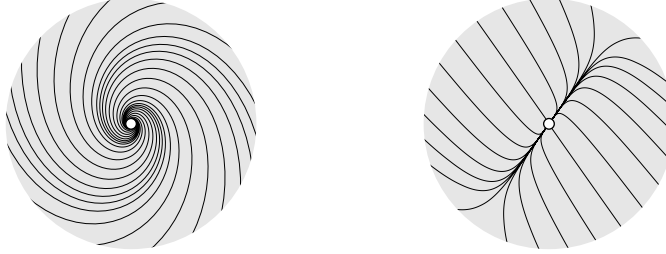


FIGURE 26. Typical nodes of  $\mathcal{F}(F)$

radial as follows.

Let  $p$  be an elliptic singularity in the interior of  $F$  and  $x, y, z$  local coordinates near  $p$  such that  $dz + x dy - y dx$  is a standard contact form, and  $(0, 0, 0)$  corresponds to  $p$ . The surface  $F$  is locally a graph of a function  $z = f(x, y)$  with a critical point at  $p$ , and we have  $df_p = 0$ .

We can modify  $f$  in a small neighborhood of  $p$  so as to make it locally constant near  $p$ . This can be done so that the new graph  $z = f(x, y)$  will have no new tangencies with the contact structure. For instance, take a small  $\varepsilon > 0$  and a  $C^\infty$ -function  $h : [0, \infty) \rightarrow [0, 1]$  such that  $h(\rho) = 0$  if  $\rho \in [0, 1/2]$ ,  $h(\rho) = 1$  if  $\rho \in [1, \infty)$ , and  $h'(\rho) > 0$  if  $\rho \in (1/2, 1)$ , and replace  $f(x, y)$  with  $\tilde{f}(x, y) = h(\rho/\varepsilon)f(x, y)$ , where  $\rho = \sqrt{x^2 + y^2}$ .

The foliation near  $p$  will become radial and no new singularity will be introduced, which can be seen as follows. New singularities occur at points  $(x, y) \neq p$  where the 1-form  $d\tilde{f}(x, y) + x dy - y dx$  vanishes, and this can only happen in the domain  $\rho \in [\varepsilon/2, \varepsilon]$ . Equivalently, new singularities correspond to the zeros of the form  $\zeta_\varepsilon = d(\frac{1}{\varepsilon^2}\tilde{f}(\varepsilon x, \varepsilon y)) + x dy - y dx$  in the domain  $\rho \in [1/2, 1]$ . Since this domain is compact, it suffices for us to show that  $\zeta_\varepsilon$  does not vanish in it in the limit  $\varepsilon \rightarrow 0$ . The function  $\lim_{\varepsilon \rightarrow 0} \tilde{f}(\varepsilon x, \varepsilon y)/\varepsilon^2$  is a quadratic form, which can be assumed, without loss of generality, to have the form  $(ax^2 + by^2)/2$ . The elliptic type of the singularity at  $p$  implies  $ab > -1$ . Now it is a direct check, which is easier if one switches to polar coordinates  $\rho, \phi$ , that the 1-form  $\lim_{\varepsilon \rightarrow 0} \zeta_\varepsilon = d(h(\rho)(ax^2 + by^2)/2) + \rho^2 d\phi$  does not vanish in the domain  $\rho \in [1/2, 1]$  if  $ab > -1$ .

If a node  $p$  occurs at  $\partial F$  we proceed similarly, but choose the coordinate system more carefully so that the two arcs of  $\partial F$  emanating from  $p$  locally have the form  $y/x = \text{const}$ ,  $z = 0$ , which is always possible.

If  $p$  is a singularity of  $\partial F$  and is not a node of  $\mathcal{F}(F)$  we proceed the same way, but this may create new singularities inside  $F$ , which should be taken care of as before.

This explains how the surface  $F'$  can be produced. In order to produce  $F''$  we need to kill circular leaves and cooriented saddle connection cycles if there are any. This is done by using Giroux’s elimination lemma in the backward direction.

Namely, let  $p$  be a point where  $F$  is transverse to the contact structure, and  $l$  a contact line element field in a tubular neighborhood of  $F$  that is transverse to  $F$ . Denote by  $s$  the leaf of  $\mathcal{F}(F)$  that comes through  $p$ . We may assume that  $l$  is transverse to  $\xi_+$  at  $p$  as this can be achieved by a small perturbation of  $l$  (if  $s$  is a closed leaf or a part of a cooriented saddle connection cycle, then actually  $l$  *must* be transverse to  $\xi_+$  along  $s$  as we will see in a moment for the case of a closed leaf).

We can rotate the tangent plane  $T_p F$  around  $s$  so that it remains transverse to  $l$  and at some moment becomes tangent to  $\xi_+$ . We then rotate it a little further, see Fig. 27. This rotation can be realized by a  $C^0$ -small deformation of  $F$  in the class of  $C^1$ -surfaces transverse to  $l$  so that two singularities, one node and one saddle, are created. They break up a closed leaf or a saddle connection cycle if one comes through  $p$ .

If  $s$  is a closed regular leaf, then this operation can be done so that no new closed leaves ‘parallel’ to  $s$  are created. Indeed, in a tubular neighborhood  $U$  of  $s$ , we can introduce a positively oriented local

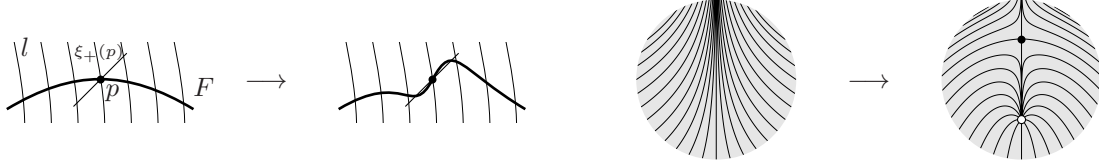


FIGURE 27. Creating a node-saddle pair of singularities

coordinate system  $(x, y, t) \in (-\varepsilon, \varepsilon) \times (-1, 1) \times \mathbb{S}^1$ , in which the surface  $F$  is defined by the equation  $x = 0$ , the leaf  $s$  by the system  $x = 0, y = 0$ , the contact line element  $l$  is  $\pm \partial_x$ , and a standard contact form  $\alpha$  can be written as  $a(y, t) dx + b(y, t) dy + c(y, t) dt$ . We will have  $c(0, t) = 0, b(0, t) \neq 0$  for all  $t \in \mathbb{S}^1$ . Without loss of generality we may assume  $b(0, t) > 0$ .

The contact condition  $\alpha \wedge d\alpha > 0$  reads

$$(10) \quad a'_t b - ab'_t + ac'_y - a'_y c > 0.$$

Whenever  $a(0, t) = 0$  we must have  $a'_t(0, t) > 0$ , which means that the sign of  $a$  can change from ‘-’ to ‘+’ but not back when  $t$  runs over the circle, hence, it does not change at all and we have  $a(0, t) \neq 0$  for all  $t$ . This means that  $l$  is transverse to  $\xi_+$  along  $s$ . By choosing a smaller neighborhood if necessary we can ensure that  $l$  is transverse to  $\xi_+$  everywhere in  $U$ .

Now we claim that there can be no other closed leaf in  $U$ . Indeed, (10) means that the 2-form  $d(\alpha/a)$ , which is well defined if  $a \neq 0$ , does not vanish in  $U \cap F$ , so by Stokes’ theorem there can be no closed curve  $s' \subset U \cap F$  such  $s$  and  $s'$  cobound an annulus and  $\alpha|_{s'} = 0$ .

This also implies that the neighborhood  $U$  can be chosen so that  $\partial U$  is transverse to the leaves of  $\mathcal{F}(F)$ . Now if we create a node-saddle pair on  $s$  as described above so that  $F \setminus U$  is untouched, then no new closed leaf can be created. Indeed, otherwise we can cancel the node-saddle pair back keeping the newly created leaf unchanged thus producing an annulus bounded by two closed leaves and such that  $l$  is transverse to  $\xi_+$  everywhere in the annulus, which is impossible.  $\square$

Let  $F$  be a surface with corners such that  $\mathcal{F}(F)$  is very nice. Suppose that  $\partial F$  is Legendrian. Then every regular leaf of  $\mathcal{F}(F)$  is an arc approaching singularities of the foliation at the ends. Indeed, we have forbidden closed leaves and saddle connection cycles that could have served as a limit cycle for a leaf.

Let  $\gamma$  be a regular leaf. Its closure  $\bar{\gamma}$  is a closed Legendrian  $C^1$ -smooth arc such that  $F$  is tangent to  $\xi_+$  at the endpoints. When  $p$  traverses  $\gamma$  the contact plane  $\xi_+(p)$  rotates relative to the tangent plane  $T_p F$  by  $-\pi, 0$ , or  $\pi$ . We express this by saying that  $\gamma$  is a  $-1$ -arc,  $0$ -arc, or  $1$ -arc, respectively.

All but finitely many leaves are those that connect two nodes. Each such leaf is a  $-1$ -arc for the (co)orientation reason. For a similar reason a leaf connecting a node to a saddle can be only a  $-1$ -arc or a  $0$ -arc. A saddle connection may be of any type,  $-1, 0$ , or  $1$ , see Fig. 28.

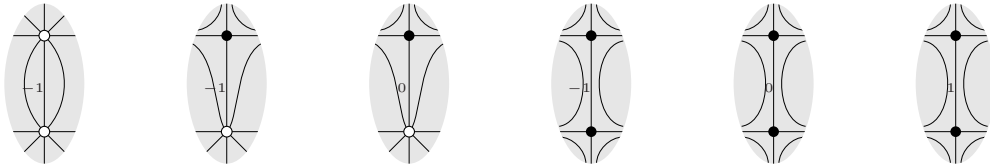


FIGURE 28. Possible types of regular leaves of a very nice foliation

The following statement gives a simple criteria for a surface to be convex if its characteristic foliation is very nice. It generalizes the similar criteria of [13] for oriented  $C^\infty$  surfaces. The criteria for weaker restrictions given in [13] can also be extended to surfaces with corners (not necessarily oriented), but we don’t need it here.

**Proposition 12.** *Let  $F$  be a surface with corners such that the characteristic foliation  $\mathcal{F}(F)$  is very nice. Then  $F$  is convex if and only if  $\mathcal{F}(F)$  has no leaf that is a 1-arc. The claim remains true if we allow  $\mathcal{F}(F)$  to have multiple saddles.*

*Proof.* The extension of Giroux's proof to surfaces with corners (and not necessarily oriented) is quite straightforward, so we give again only a sketch.

First, we show that the presence of a 1-arc among the leaves of  $\mathcal{F}(F)$  means that the surface  $F$  is not convex. Let  $\gamma$  be such an arc endowed with a regular parametrization. Assume that there exists a contact vector field  $X$  transverse to  $F$  in a small neighborhood of  $\gamma$ . Denote by  $\alpha$  a standard contact form.

After a small perturbation if necessary we may ensure that 0 is not a critical value of the function  $f = \alpha(X)$  restricted to  $\gamma$ . The rotation of the contact plane by  $\pi$  relative to the tangent plane means that at some point of  $\gamma$  the function  $f$  vanishes, since it is positive at one end of  $\gamma$  and negative at the other. This occurs if and only if the plane  $\langle \dot{\gamma}, X \rangle$  spanned by  $\dot{\gamma}$  and  $X$  becomes contact.

Since  $\gamma$  is a Legendrian arc, we get from (9):  $d\alpha(X, \dot{\gamma}) + df(\dot{\gamma}) = 0$ . Opposite signs of the summands in the left hand side at the moment when  $f = 0$  correspond to rotation of the contact plane relative to the plane  $\langle \dot{\gamma}, X \rangle$  in the negative direction. The total rotation with respect to the plane  $\langle \dot{\gamma}, X \rangle$ , therefore, must be smaller than  $\pi$ , which is incompatible with rotation by  $\pi$  relative to the tangent plane, which remains transverse to  $\langle \dot{\gamma}, X \rangle$ . A contradiction.

Now we proceed with the proof that the absence of 1-arcs is sufficient for the surface  $F$  to be convex if the foliation  $\mathcal{F}(F)$  is very nice.

Denote by  $\mathcal{G} = \mathcal{G}(F)$  the union of all the singularities and 0-arcs of  $\mathcal{F}(F)$ . Let  $\alpha$  be a standard contact form.

Denote by  $F'$  a small tubular neighborhood of  $\mathcal{G}(F)$  in  $F$ . The coorientations induced by  $\xi_+$  at singularities of  $\mathcal{F}$  lying in the same connected component of  $F'$  agree along any path connecting them, which is by construction, hence  $F'$  is orientable even if  $F$  is not. We choose the orientation of  $F'$  so that the form  $d\alpha$  is positive at the singularities of  $\mathcal{F}$ . (This is possible since the form  $\alpha \wedge d\alpha$  never vanishes, so  $d\alpha$  defines an orientation of contact planes that agrees with their coorientation.) Let  $\omega$  be an orientation form on  $F'$ .

We orient each 0-arc so that if  $u$  is a positive tangent vector to the arc then the coorientation of the arc defined by  $\omega(u, \cdot)$  coincides with the coorientation of this arc as a leaf of  $\mathcal{F}$ .

Now we choose a smooth function  $g : \mathbb{S}^3 \rightarrow [1, \infty)$  whose restriction to each 0-arc is a regular monotonic function increasing in the positive direction. This is possible because the oriented 0-arcs form no oriented cycle. Indeed, an oriented saddle connection cycle cannot occur by the definition of a very nice foliation. If a cycle contains at least one node, then the two arcs in it emanating from the node have opposite orientations. This is because a 0-arc connecting an elliptic singularity to a saddle is always oriented toward the saddle.

One can now show that the restriction of the 2-form  $d(\exp(\mu g)\alpha)$  does not vanish at  $\mathcal{G}$  if  $\mu > 0$  is a large enough constant. We replace  $\alpha$  by  $\exp(\mu g)\alpha$  and  $F'$  by a possibly smaller neighborhood of  $\mathcal{G}$  in  $F$  such that  $d\alpha$  (for the new  $\alpha$ ) does not vanish in  $\overline{F'}$ .

Since there are no 1-arcs, the surface  $F \setminus \mathcal{G}(F)$  is foliated by  $-1$ -arcs, and the closure of each has both endpoints in  $\mathcal{G}(F)$ . This implies that the surface  $F'$  can be chosen so as to satisfy an additional restriction that  $\partial F'$  is transverse to  $\mathcal{F}(F)$ .

Recall that for any smooth function  $f : \mathbb{S}^3 \rightarrow \mathbb{R}$  there exists a unique contact vector field  $X$  such that  $\alpha(X) = f$ , see (9). We denote this vector field by  $X_f$ .

It is possible to find a smooth function  $\mathbb{S}^3 \rightarrow \mathbb{R}$  such that:

- (1)  $f(p) = 1$  if  $p \in F'$ ;
- (2) for any  $-1$ -arc  $\gamma$  the restriction of  $f$  to  $\gamma \setminus \overline{F'}$  has a single critical point, which is a non-degenerate local minimum, and the critical value is 0.

The contact line element field  $X_{\pm \sinh(\nu\sqrt{f})}$  for large enough  $\nu$  is then transverse to  $F$ . □



Now we have a look at the characteristic foliation of the surface  $\widehat{\Pi}$ , where  $\Pi$  is a rectangular diagram of a surface. This foliation is never nice as  $\widehat{\Pi}$  is tangent to  $\xi_+$  along a 1-dimensional subcomplex. We can fix this by a small perturbation of the surface that can be specified explicitly.

Define  $\widehat{r}^\kappa$  and  $\widehat{\Pi}^\kappa$  in the same way as  $\widehat{r}$  and  $\widehat{\Pi}$  in Definition 9 with the function  $\widetilde{h}_r$  replaced by

$$\widetilde{h}_r(v) = (2/\pi) \arctan(\tan(\pi h_r(v)/2))^{1/(2+\kappa)}.$$

*Remark 8.* The surface  $\widehat{\Pi} = \widehat{\Pi}^0$  is typically of class  $C^1$  only, whereas  $\widehat{\Pi}^\kappa$  is  $C^2$  for  $\kappa > 0$ .

**Proposition 13.** *For any rectangular diagram of a surface  $\Pi$  and any  $\kappa > 0$  the characteristic foliation of  $\widehat{\Pi}^\kappa$  is very nice and has no 1-arcs. If  $\kappa = 0$  it has no 1-arcs either.*

*Proof.* Let  $r = [\theta_1, \theta_2] \times [\varphi_1, \varphi_2]$  be a rectangle from  $\Pi$ . Denote  $a = (\theta_1, \varphi_1)$ ,  $b = (\theta_2, \varphi_1)$ ,  $c = (\theta_2, \varphi_2)$ ,  $d = (\theta_1, \varphi_2)$ . For any  $\kappa \geq 0$  the disc  $\widehat{r}^\kappa$  is transverse to all arcs  $\widehat{v}$  with  $v \in \text{int}(r)$ . So, there are no singularities of  $\mathcal{F}(\widehat{r}^\kappa)$  in the interior of  $\widehat{r}^\kappa$ .

Along the arcs  $\widehat{a}, \widehat{c} \subset \partial\widehat{r}^\kappa$  the disc  $\widehat{r}^\kappa$  is tangent to the plane field

$$(11) \quad \xi_-^\kappa = \ker(\cos^{2+\kappa}(\pi\tau/2) d\varphi - \sin^{2+\kappa}(\pi\tau/2) d\theta),$$

which is transverse to  $\xi_+$  outside of  $\mathbb{S}_{\tau=0}^1 \cup \mathbb{S}_{\tau=1}^1$  and make a  $\pi$ -twist relative to  $\xi_+$  along arcs of the form  $\widehat{v}$ ,  $v \in \mathbb{T}^2$ . Thus,  $\widehat{a}$  and  $\widehat{c}$  are  $-1$ -arcs.

Along the arcs  $\widehat{b}$  and  $\widehat{d}$  the disc  $\widehat{r}^\kappa$  is tangent to the plane field

$$(12) \quad \xi_+^\kappa = \ker(\cos^{2+\kappa}(\pi\tau/2) d\varphi + \sin^{2+\kappa}(\pi\tau/2) d\theta).$$

If  $\kappa > 0$ , then this field coincides with  $\xi_+$  only at the endpoints and in the middle of any arc of the form  $\widehat{v}$ . The rotation of the field relative to  $\xi_+$  along each half of  $\widehat{v}$  is zero, so, each of  $\widehat{b}$  and  $\widehat{d}$  consists of the closures of two 0-arcs.

To see the structure of  $\mathcal{F}(\widehat{r}^\kappa)$  in the interior of  $\widehat{r}^\kappa$  it is useful to apply the torus projection, see Fig. 29. The obtained foliation in  $\text{int}(r)$  is tangent to the line field in  $r \subset \mathbb{T}^2$ :

$$\ker\left(\cos^{\frac{2}{2+\kappa}}((\pi/2)h_r(\theta, \varphi)) d\varphi + \sin^{\frac{2}{2+\kappa}}((\pi/2)h_r(\theta, \varphi)) d\theta\right).$$

All the leaves have negative slope that tends to 0 when the leaf approaches a horizontal side of  $r$  (away of the endpoints of the side) and to  $\infty$  when the leaf approaches a vertical side. If  $\kappa > 0$  all leaves, except

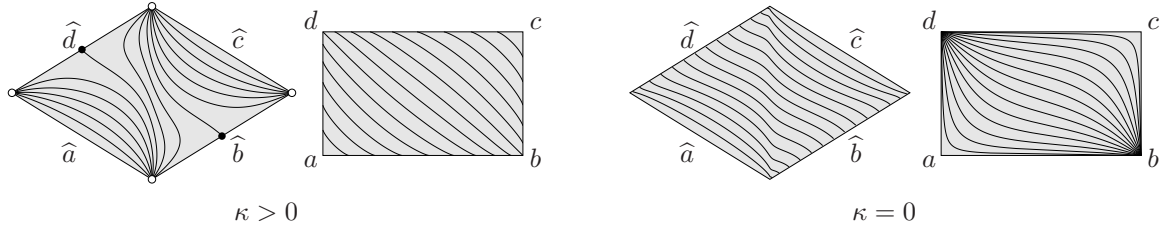


FIGURE 29. Foliation  $\mathcal{F}(\widehat{r}^\kappa)$  and its torus projection

two or one, end up on internal points of the sides of  $r$ , and the exceptional leaves approach the corners  $b$  or  $d$  and have the slope  $-1$  in the limit. If  $\kappa = 0$  all the leaves approach corners  $b$  and  $d$  at different angles.

For the foliation  $\mathcal{F}(\widehat{r}^\kappa)$ , in the case  $\kappa > 0$ , this means that it has nodes at the corners of  $\widehat{r}^\kappa$  and saddles in the middle of the arcs  $\widehat{b}$  and  $\widehat{d}$ . All the arcs in the interior of  $\widehat{r}^\kappa$ , except two or one separatrices connect an endpoint of  $\widehat{b}$  with an endpoint of  $\widehat{d}$ .

If  $\kappa = 0$  the sides  $\widehat{b}$  and  $\widehat{d}$  consist of singularities by whole, and the rest of the tile  $\widehat{r}$  is foliated by arcs with one endpoint at  $\widehat{b}$  and the other at  $\widehat{d}$ .

In both cases all the leaves in the interior of  $\widehat{r}^\kappa$  are  $-1$  arcs. This is because the closure of such a leaf is isotopic to  $\widehat{a}$  in the class of Legendrian curves in  $\widehat{r}^\kappa$  with endpoints at singularities or at 0-arcs.  $\square$

**4.4. The Giroux graph and dividing curves.** Let  $F$  be a convex surface with corners such that the characteristic foliation  $\mathcal{F}(F)$  is very nice.

**Definition 27.** The union  $\mathcal{G}(F)$  of singularities and 0-arcs of  $\mathcal{F}(F)$  introduced in the proof of Proposition 12 is called *the Giroux graph of  $F$* .

A union  $\tilde{\mathcal{G}}$  of the Giroux graph with a finite collection of  $-1$ -arcs such that  $F \setminus \tilde{\mathcal{G}}$  is a union of pairwise disjoint open discs will be called *an extended Giroux graph of  $F$* .

Clearly, both the Giroux graph and any extended Giroux graph are Legendrian graphs. The fact that the complement to the Giroux graph is foliated by  $-1$ -arcs implies that  $F \setminus \mathcal{G}(F)$  is a union of pairwise disjoint open annuli, open Möbius bands, and strips homeomorphic to  $(0, 1) \times [0, 1]$ . Each of them can be cut into discs, so, we have the following.

**Proposition 14.** *If the foliation  $\mathcal{F}(F)$  is very nice, then there exists an extended Giroux graph. Any extended Giroux graph contains  $\partial F$ .*

Another important thing that can be easily seen is that there is a collection  $\beta_1, \dots, \beta_k$  of simple closed curves and proper arcs (meaning:  $\beta_i \cap \partial F = \partial \beta_i$ ) in  $F$  such that:

- (1) for each  $i = 1, \dots, k$ , the curve  $\beta_i$  is transverse to the standard contact structure;
- (2) every  $-1$ -arc of  $\mathcal{F}(F)$  intersects  $\cup_{i=1}^k \beta_i$  exactly once.

Such curves  $\beta_i$  are called *the dividing curves of  $\mathcal{F}(F)$* .

*Remark 9.* Dividing curves can be defined for any convex surface, even if the characteristic foliation is not nice. A full collection of dividing curves can be obtained as follows. Take a generic contact line element field transverse to the surface, and the points where the field is tangent to the contact structure will cut the surface along a full family of dividing curves. See details in [13].

While the equivalence class of the Giroux graph viewed as a Legendrian graph can easily change (which will be explored below) when a surface is isotoped in the class of convex surfaces, the isotopy class of dividing curves is an invariant of such an isotopy [13].

*Remark 10.* Legendrian graphs viewed up to transformations that can occur to the Giroux graph are precisely the subject of the paper [29], though the relation to Giroux graphs is not noticed there. We will address this relation in a subsequent paper.

We endow the dividing curves with a *canonical orientation* induced by the coorientation of the contact structure.

*Remark 11.* Typically, one assumes the surface  $F$  to be oriented, so the Giroux graph falls naturally into two disjoint subgraphs, positive and negative, depending on whether the orientation of the surface coincides with the orientation of the contact structure at the singularities of the foliation. Each dividing curve separates a positive component of  $\mathcal{G}(F)$  from a negative one and thus is endowed with a *coorientation*.

If we consider non-oriented surfaces a dividing curve may be a core of a Möbius band, but the canonical orientation of all dividing curves is always well defined.

To see an example we look again at the surface  $\widehat{\Pi}^\kappa$ , where  $\Pi$  is a rectangular diagram of a surface and  $\kappa > 0$ . An extended Giroux graph of  $\widehat{\Pi}^\kappa$  can be obtained by taking  $\widehat{G}$ , where  $G$  is the set of all vertices of rectangles in  $\Pi$ . If  $r = [\theta_1, \theta_2] \times [\varphi_1, \varphi_2]$  is a rectangle from  $\Pi$ , then  $(\widehat{\theta_1, \varphi_2})$  and  $(\widehat{\theta_2, \varphi_1})$  are two edges of the Giroux graph. The torus projection of a dividing curve passing through  $\widehat{r}^\kappa$  must go from  $(\theta_1, \varphi_1)$  to  $(\theta_2, \varphi_2)$ , see Fig. 30.

**4.5. Proof of part (ii) of Theorem 2.** We prove a more general statement of which Theorem 2 is a partial case. Instead of a link we will consider a general Legendrian graph to which the surface is attached in a ‘nice’ way, which we now define.

**Definition 28.** Let  $\Gamma$  be a Legendrian graph and  $F$  a surface with corners. We say that  $F$  is *properly attached to  $\Gamma$*  if  $F \cap \Gamma$  is a sublink of  $\partial F$  and for any  $p \in \partial F$  the projection of  $F \cup \Gamma$  to the contact plane  $\xi_+(p)$  along a vector field transverse to  $F$  is locally an injection.



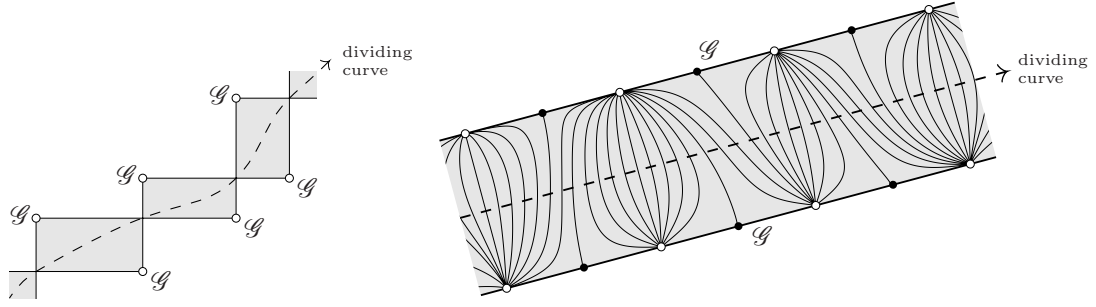


FIGURE 30. The Giroux graph and a dividing curve on a torus projection (left) and the surface  $\hat{\Pi}^\kappa$  itself (right)

**Definition 29.** Let  $\Gamma_0, \Gamma_1$  be Legendrian graphs and  $F_0, F_1$  convex surfaces with corners that are properly attached to  $\Gamma_0$  and  $\Gamma_1$ , respectively. We say that the pairs  $(F_0, \Gamma_0)$  and  $(F_1, \Gamma_1)$  are *equivalent* if there is an isotopy from  $F_0 \cup \Gamma_0$  to  $F_1 \cup \Gamma_1$  whose restriction to  $\Gamma_0$  satisfies conditions (a)–(d) from Proposition 7, and to  $F_0$  conditions from Definition 25.

Let  $F$  be a surface with corners properly attached to a Legendrian graph  $\Gamma$ . Let  $\gamma \subset \partial F$  be a simple arc such that  $\partial\gamma \in \overline{\Gamma \setminus \partial F}$ . Then  $F$  is tangent to  $\xi_+$  at the endpoints of  $\gamma$ . So, when  $p$  traverses  $\gamma$  the angle of rotation of  $\xi_+(p)$  relative to  $T_p F$  will be a multiple of  $\pi$ . We call this angle divided by  $2\pi$  the *Thurston–Bennequin number of  $\gamma$  relative to  $F$  and  $\Gamma$*  and denote by  $\text{tb}_+(\gamma; F, \Gamma)$ .

If  $\gamma \subset \mathbb{S}^3$  is an arc or simple closed curve of the form  $\hat{X}$  with  $X$  a finite subset of  $\mathbb{T}^2$ , then  $|X|$  will be referred to as *the length of  $\gamma$* .

**Proposition 15.** Let  $F$  be a convex surface properly attached to a Legendrian graph  $\Gamma$ . Let  $G$  be a rectangular diagram of a graph such that  $\hat{G}$  and  $\Gamma$  are equivalent. Suppose that, for any arc  $\gamma \subset \partial F \cap \Gamma$  such that  $\partial\gamma \in \overline{\Gamma \setminus \partial F}$ , the respective arc in  $\hat{G}$  has length not smaller than  $-2\text{tb}_+(\gamma; F, \Gamma)$ . Suppose the same holds for any connected component  $\gamma$  of the link  $\Gamma \cap \partial F$  (one should use  $\text{tb}_+(\gamma; F)$  instead of  $\text{tb}_+(\gamma; F, \Gamma)$ ).

Then there exists a rectangular diagram of a surface  $\Pi$  such that the pairs  $(\hat{\Pi}, \hat{G})$  and  $(F, \Gamma)$  are equivalent.

*Proof.* We will find an isotopy from the given surface  $F$  to a ‘rectangular’ surface. The isotopy will be defined simultaneously for  $\Gamma$  so as to realize the equivalence between  $(F, \Gamma)$  and  $(\hat{\Pi}, \hat{G})$ .

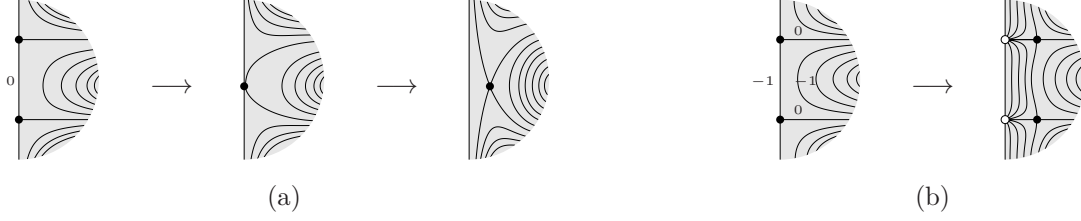
*Step 1.* Deform  $F$  slightly keeping  $\Gamma$  and  $\partial F$  fixed so that  $\mathcal{F}(F)$  becomes very nice and  $F$  remain convex during the deformation. We can do this by Proposition 11.

*Step 2.* Eliminate all saddle connections and also  $-1$ -arcs in  $\partial F$  connecting a saddle to a node.

If a saddle connection occurs in the interior of  $F$ , then it is eliminated by a generic  $C^1$ -small perturbation of  $F$ , so there is no problem to keep  $F$  within the class of convex surfaces during the deformation.

If a saddle connection occurs at  $\partial F$ , and it is a  $0$ -arc, then it can be eliminated by twisting  $F$  around this arc. By Proposition 12, to see that the surface remains convex during the deformation, which is only  $C^0$ -small, it suffices to show that: (i) the foliation remains very nice all the time except a single moment when a multiple saddle is created; (ii) no  $1$ -arc is produced. The former is easy to ensure. The latter is true if the deformation is supported in a small enough neighborhood of the  $0$ -arc because all leaves that come close to the scene approach a node at the other end, so, they cannot eventually turn into a  $1$ -arc (which must connect two saddles) or a closed cycle. The evolution of the foliation is shown in Fig. 31 (a).

Now assume that we have a saddle connection in  $\partial F$  which is a  $-1$ -arc. Denote it by  $\gamma$ . Let  $s_1$  and  $s_2$  be the saddles connected by  $\gamma$ . Leaves of  $\mathcal{F}(F)$  passing by close enough to  $\gamma$  must proceed to nodes at both ends. So, they are also  $-1$ -arcs. This implies that two separatrices from  $s_1$  and  $s_2$  lying in the

FIGURE 31. Eliminating saddle connections at  $\partial F$ 

interior of  $F$  are 0-arcs. A small twist of the surface around a portion of these separatrices near  $s_1$  and  $s_2$  will shift the saddles off the boundary creating two boundary nodes instead, see Fig. 31 (b).

$-1$ -arcs in  $\partial F$  connecting a saddle to a node are eliminated similarly.

Now the Giroux graph of  $\mathcal{F}(F)$  has a very simple structure. Leaves passing by a saddle that are not separatrices must be  $-1$ -arcs. It can be seen from this that two separatrices emanating from it in opposite directions must be 0-arcs and the other two separatrices (or just one if the saddle lies at the boundary)  $-1$ -arcs, see Fig. 32.

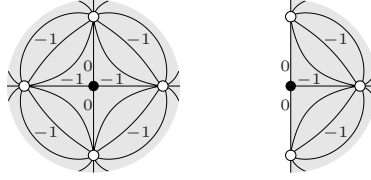


FIGURE 32. Foliation around saddles after simplification

Thus, the Giroux graph consists of nodes, which are vertices, connected by smooth arcs each composed of two 0-arcs and a saddle in the middle, which are edged, see Fig. 33. We will express this by saying that

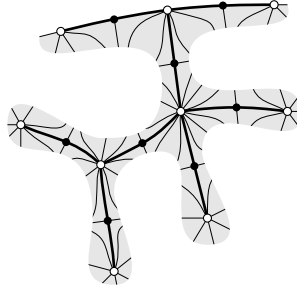


FIGURE 33. Simple Giroux graph

the Giroux graph is *simple*. From now on we will keep the Giroux graph simple except at finitely many moments when an elliptic-saddle pair is created or eliminated by an application of Giroux's elimination lemma.

*Step 3.* Now we've got some freedom, which we use to take  $\Gamma$  to  $\widehat{G}$ .

By varying  $F$  in the class of convex surfaces and using Giroux' elimination lemma we can: subdivide edges of the Giroux graph; subdivide a  $-1$ -arc into a smaller  $-1$ -arc and two 0-arcs whose closure become a new edge of the Giroux graph; eliminate two-valent vertices of the Giroux graph; eliminate one-valent vertices together with the adjacent edges; move vertices of  $\mathcal{G}$  along the boundary unless they belong to  $\Gamma \setminus \partial F \cap \partial F$ . All this can be done without altering  $\partial F \cup \Gamma$ . Here is one more thing we can do:

**Lemma 5.** *Let  $\Gamma'$  and  $\mathcal{G}'$  be Legendrian graphs such that  $\Gamma' \cup \mathcal{G}'$  is obtained by an angle adjustment from  $\Gamma \cup \mathcal{G}$  so that  $\Gamma$  is taken to  $\Gamma'$  and  $\mathcal{G}$  to  $\mathcal{G}'$ . Then there exists a convex surface with corners  $F'$  such that the pair  $(F, \Gamma)$  is equivalent to  $(F', \Gamma')$ , and  $\mathcal{G}'$  is the Giroux graph of  $F'$ .*

*Proof.* The idea of the proof is pretty much the same as that of Proposition 6. Consider again a small cylindrical neighborhood of an elliptic singularity  $p$  of  $\mathcal{F}(F)$  with a local coordinate system  $x, y, z$  such that  $p = (0, 0, 0)$  and  $dz + x dy - y dx$  is a standard contact form. The intersection of  $F \cup \Gamma$  with a small neighborhood of  $p$  can be recovered uniquely from the projection of  $\Gamma$  and of the foliation  $\mathcal{F}(F)$  to the  $xy$ -plane and the knowledge of the rest of  $F$  and  $\Gamma$ .

The changes of the  $xy$ -projection of  $\mathcal{F}(F)$  and  $\Gamma$  that can occur as the result of a small allowed deformation of  $F \cup \Gamma$  include those that can be achieved by applying an area preserving homeomorphism  $\phi$  of the  $xy$ -plane such that:

- (1)  $\phi$  is identity outside of a small neighborhood of  $p$  and  $C^0$ -close to identity in this neighborhood;
- (2)  $\phi$  is smooth outside of the origin and has definite directional derivatives at the origin.

Note that if  $p$  lies in the interior of  $F$  non-smoothness of  $\phi$  does not mean that the change of  $F$  cannot be realized by a smooth isotopy. We don't need the isotopy to be leafwise, so, each point of  $F$  can simply move along the  $z$ -axis while angles between the leaves will be changing.

Such homeomorphisms  $\phi$  have enough freedom to realize an angle adjustment between finitely many leaves of  $\mathcal{F}(F)$  and edges of  $\Gamma$  at  $p$ .  $\square$

By a  $C^1$ -small deformation of  $F$  near the points from  $\overline{\Gamma \setminus F} \cap \partial F$  we can make these points nodes of  $\mathcal{F}(F)$ . Then we use Lemma 5 to smoothen the boundary of  $F$ . The graphs  $\Gamma$  and  $\widehat{G}$  are still equivalent, so, we can obtain  $\widehat{G}$  from  $\Gamma$  by an angle adjustment followed by a contactomorphisms. Angle adjustment is necessary only at the points of  $\Gamma$  that will be mapped to vertices of  $\widehat{G}$  (lying at  $\mathbb{S}_{\tau=0}^1 \cup \mathbb{S}_{\tau=1}^1$ ).

Let  $q_1, \dots, q_N \in \Gamma$  be these points. The bound on the lengths of certain arcs and simple closed curves in  $\widehat{G}$  included in the assumption of Proposition 15 guarantees that there are enough points  $q_i$  on respective arcs and simple closed curves in  $\Gamma$  to allow us to move the boundary nodes of  $\mathcal{F}(F)$  along  $\partial F$  so that any connected component of  $\partial F \setminus \{q_1, \dots, q_N\}$  has a non-empty intersection with at most one  $-1$ -arc. We can also make all  $q_i$ 's nodes either by moving the existing nodes along  $\partial F$  or creating new ones.

Now we use Lemma 5 again to do an angle adjustments in  $q_i$ 's after which that the graph  $\Gamma$  can be taken to  $\widehat{G}$  by a contactomorphism. By Eliashberg's theorem [7] the group of contactomorphisms of  $\mathbb{S}^3$  is connected. So,  $(F, \Gamma)$  can be deformed in the allowed manner so that we get  $\Gamma = \widehat{G}$ , which is assumed in the sequel.

*Step 4.* Eliminate unnecessary nodes at  $\partial F$ .

Each arc of the form  $\widehat{v}$ ,  $v \in \mathbb{T}^2$ , in  $\Gamma$  contains at most one  $-1$ -arc and some number of  $0$ -arcs. All nodes in  $\text{int}(\widehat{v})$  should be eliminated, thus making  $\text{int}(\widehat{v})$  a single  $0$ - or  $-1$ -arc. Note that this does not require  $F$  to be altered near the endpoints of  $\widehat{v}$ .

*Step 5.* Choose an extended Giroux graph  $\widetilde{\mathcal{G}}$  and make it 'rectangular'.

We choose  $\widetilde{\mathcal{G}}$  by adding to  $\mathcal{G}$  some  $-1$ -arcs connecting nodes. Those nodes may appear only at  $\mathbb{S}_{\tau=0}^1 \cup \mathbb{S}_{\tau=1}^1$ . Then we find a rectangular diagram of a graph  $G_1$  such that the graph  $\widetilde{\mathcal{G}} \setminus \Gamma$  is equivalent to  $\widehat{G}_1$  relative to  $\Gamma = \widehat{G}$ . It exists by Proposition 8. In the same manner as in Step 3 we can deform  $\widetilde{\mathcal{G}} \setminus \Gamma$  to  $\widehat{G}_1$  simultaneously with  $F$  so that  $\Gamma$  is preserved. To do so we may need to subdivide some  $-1$ -arcs that we included in  $\widetilde{\mathcal{G}}$ . This will create new  $0$ -arcs, which will then be included in  $\mathcal{G}$ .

Thus, from now on we assume that  $\Gamma = \widehat{G}$  and that the extended Giroux graph  $\widetilde{\mathcal{G}}$  has the form  $\widehat{G}'$  for some  $G' \subset \mathbb{T}^2$ . We eliminate all unnecessary nodes in  $\widetilde{\mathcal{G}}$ , so that each arc of the form  $\widehat{v}$ ,  $v \in G'$ , becomes a  $0$ -arc or a  $-1$ -arc.

*Step 6.* Deform  $F$  to a surface of the form  $\widehat{\Pi}^\kappa$ .

Pick a  $\kappa > 0$ . We twist  $F$  around the boundary so as to make it tangent to  $\xi_+^\kappa$  along  $0$ -arcs in  $\widetilde{\mathcal{G}}$  and to  $\xi_-^\kappa$  along  $-1$ -arcs (the plane fields  $\xi_\pm^\kappa$  are defined by (11) and (12)). This can be done without creating

or eliminating any singularity because the tangent plane to  $F$  and the corresponding field  $\xi_{\pm}^{\kappa}$  already have similar ‘qualitative behavior’ along each edge of  $\tilde{\mathcal{G}}$ .

Now by Proposition 5, in which we can seamlessly replace  $\hat{\Pi}$  by  $\hat{\Pi}^{\kappa}$ , there exists a rectangular diagram of a surface  $\Pi$  and an isotopy from  $F$  to  $\hat{\Pi}^{\kappa}$  that is fixed at  $\Gamma \cup \tilde{\mathcal{G}}$  and preserves the tangent plane to the surface at any point  $p \in \tilde{\mathcal{G}}$ .

We recall that  $F \setminus \tilde{\mathcal{G}}$  is a union of open discs, hence so is  $\hat{\Pi}^{\kappa} \setminus \tilde{\mathcal{G}}$ . Moreover, both surfaces  $F$  and  $\hat{\Pi}^{\kappa}$  are convex, and all the discs in  $F \setminus \tilde{\mathcal{G}}$  and  $\hat{\Pi}^{\kappa} \setminus \tilde{\mathcal{G}}$  are foliated by  $-1$ -arcs.

Since the tangent planes to  $F$  at  $\tilde{\mathcal{G}}$  are kept fixed during the isotopy  $F \rightsquigarrow \hat{\Pi}^{\kappa}$  the latter can be decomposed into a sequence of isotopies

$$(13) \quad F = F_0 \rightsquigarrow F_1 \rightsquigarrow \dots \rightsquigarrow F_n = \hat{\Pi}^{\kappa}$$

such that each of them alters only one of the discs in  $F_i \setminus \tilde{\mathcal{G}}$ . Let  $D \subset F$  be the closure of one of the discs  $F \setminus \tilde{\mathcal{G}}$ , and  $D'$  the respective disc in  $\hat{\Pi}^{\kappa}$ . (Strictly speaking, the boundary of  $D$  may not be a simple curve, hence  $D$  may not be a disc, but the reasoning below can be generalized straightforwardly, so we keep assuming it to be a disc.) So far we have a sequence of isotopies

$$(14) \quad D = D_0 \rightsquigarrow D_1 \rightsquigarrow \dots \rightsquigarrow D_m = D'$$

each of which realizes a single isotopy in the sequence (13). Let  $D_{i-1} \rightsquigarrow D_i$  correspond to  $F_{j_{i-1}} \rightsquigarrow F_{j_i}$ .

By decomposing further isotopies in (14) to ‘smaller’ ones if necessary we can assume, for each  $i = 1, \dots, m$ , the existence of an open ball  $B_i$  such that

- (1)  $\overline{B_i} \cap (F_{j_{i-1}} \cup \Gamma) = D_{i-1}$ ,  $\overline{B_i} \cap (F_{j_i} \cup \Gamma) = D_i$ ,  $D_{i-1} \cap \partial B_i = D_i \cap \partial B_i = \partial D$ ;
- (2) the isotopy  $D_{i-1} \rightsquigarrow D_i$  takes place inside  $B_i$  (i.e. no point of the interior of the disc escapes  $B_i$ ).

Having fixed such balls we are going to modify the isotopies so that these properties still hold. The new isotopies will then compile into an isotopy  $F \rightsquigarrow \hat{\Pi}^{\kappa}$ . All isotopies of the discs will be assumed to be fixed at  $\tilde{\mathcal{G}}$  and to keep unchanged the tangent planes to  $F$  at  $\tilde{\mathcal{G}}$ .

We can replace each isotopy  $D_{i-1} \rightsquigarrow D_i$  by composition of two successive isotopies  $D_{i-1} \rightsquigarrow D'_i \rightsquigarrow D_i$  so that  $D_{i-1} \cap D'_i = D_i \cap D'_i = \partial D$ . This is done by ‘a back and forth trick’: the first isotopy pushes the disc toward  $\partial B_i$  (either way of the two) and the second moves it back and then to  $D_i$ . Thus, without loss of generality we can assume from the beginning that  $D_{i-1} \cap D_i = \partial D$ .

Now alter each of  $D_i$  if necessary so as to make all these discs convex and the foliation  $\mathcal{F}(D_i)$  very nice. This can be done without violating the condition  $D_{i-1} \cap D_i = \partial D$  and so that the alteration of  $D_i$  takes place in  $B_i \cap B_{i+1}$ .

By another similar alteration we can eliminate all singularities of  $\mathcal{F}(D_i)$  from  $\text{int}(D_i)$ . There is no obstruction to elimination a node-saddle pair in  $\text{int}(D_i)$  because the corresponding deformation occurs in a small neighborhood of a 0-arc connecting the pair in  $\text{int}(D_i)$ . Any node in  $\text{int}(D_i)$  must be connected by a 0-arc to a saddle in  $\text{int}(D_i)$ , so, we can eliminate all nodes in  $\text{int}(D_i)$ . We claim that this will also eliminate all saddles.

Indeed,  $\partial D$  consists of four consecutive arcs  $\beta_1, \beta_2, \beta_3, \beta_4$ , say, such that  $\beta_1, \beta_3 \subset \mathcal{G}(D)$  and  $\text{int}(\beta_2), \text{int}(\beta_4)$  are  $-1$ -arcs. Since the tangent planes at  $\partial D$  are untouched during the isotopies the same is true for  $D_i$ . If a saddle remains in  $\text{int}(D_i)$  after eliminating the vertices there must be an edge  $\gamma$  of  $\mathcal{G}(D_i)$  connecting two points in  $\beta_1 \cup \beta_3$ . If  $\gamma$  connects a point in  $\beta_1$  to a point in  $\beta_3$ , then it cuts  $D_i$  into halves such that the boundary of each of them contains exactly one  $-1$ -arc and some number of 0-arcs, which is impossible. If  $\gamma$  connects two points in  $\beta_1$  (or in  $\beta_3$ ), then it cuts off an overtwisted disc (a disc whose boundary has zero relative Thurston–Bennequin number), which is also a contradiction by a well known result of Bennequin [1].

Thus,  $\mathcal{F}(D_i)$  has no singularities in  $\text{int}(D_i)$ . It also has no closed leaf since such a leaf would also cut off an overtwisted disc. Application of Lemma 6 proven below completes the construction of an isotopy  $F \rightsquigarrow \hat{\Pi}^{\kappa}$  that realized the equivalence of  $(F, \hat{G})$  and  $(\hat{\Pi}^{\kappa}, \hat{G})$ .

*Step 7.* Now we isotop  $\hat{\Pi}^{\kappa}$  to  $\hat{\Pi}$  simply by moving  $\kappa$  to 0. □

**Lemma 6.** *Let  $D_0, D_1$  be two discs with corners such that*

- (1) the discs  $D_0$  and  $D_1$  have common boundary and the same tangent planes along it;
- (2) the interiors of  $D_0$  and  $D_1$  are disjoint;
- (3)  $D_0$  and  $D_1$  approach  $\partial D_0 = \partial D_1$  from the same side;
- (4) the characteristic foliations of both are very nice and have no singularities in the interior.

Then there exists an isotopy  $\psi : [0, 1] \times D_0 \rightarrow \mathbb{S}^3$  such that  $\psi_0 = \text{id}|_{D_0}$ ,  $\psi_1(D_0) = D_1$ , and, for any  $t \in (0, 1)$ , the disc  $D_t = \psi_t(D_0)$  is convex, and we have  $D_t \cap D_0 = D_t \cap D_1 = \partial D_t$ .

The last condition implies that  $\partial D_t$  remains unchanged, and  $D_t$  remains ‘in between’ the discs  $D_0$  and  $D_1$  and have the same tangent planes at  $\partial D_t$ .

*Proof.* The proof is based on classical arguments [7, 16, 15, 25] though we could not find exactly this statement (even for discs with smooth boundary). We will again be sketchy.

First, we pick an isotopy  $\psi$  from  $D_0$  to  $D_1$  such that  $D_{t'} \cap D_{t''} = \partial D_0$  for any  $t' \neq t''$ , where  $D_t = \psi_t(D_0)$ . In other words, the discs are deformed in the transverse direction when  $t$  changes. By choosing a generic isotopy we can ensure that all but finitely many discs  $D_t$ ,  $t \in (0, 1)$  have a nice characteristic foliation, and the exceptional moments correspond to a birth or death of a node-saddle pair. The singularity at such a moment can be viewed as a saddle of multiplicity 0, so it cannot be a reason for the corresponding disc to be non-convex.

The only possible reasons for  $D_t$  not to be convex by Proposition 12 are:

- (1)  $D_t$  contains a closed leaf or a cooriented saddle connection cycle, and hence, its characteristic foliation is not very nice;
- (2)  $\mathcal{F}(D_t)$  contains a 1-arc.

A closed leaf or a cooriented saddle connection cycle cannot appear in a disc because otherwise it cuts off an overtwisted disc, which is impossible.

So, we are left with a 1-arc as the only origin of non-convexity. A small transverse deformation always resolves a 1-arc, so there can be only finitely many moments when a 1-arc occurs. Moreover, to get a 1-arc resolution it is enough to make a transverse deformation in a small neighborhood of any point of the arc.

Let  $t = t_0$  be such a moment, and  $\gamma$  be a 1-arc in  $D_{t_0}$ . We can assume that it is the only 1-arc in  $D_{t_0}$  as this is achieved by a small perturbation of the isotopy. Let  $B$  be a ball intersecting  $\gamma$  such that  $\overline{B}$  is disjoint from any 0-arc in  $D_{t_0}$  and from  $\partial \gamma$ .

We can modify our isotopy slightly for the moments  $t \in [t_0 - 2\delta, t_0 + 2\delta]$ , where  $\delta > 0$  is small, so that  $D_t \setminus B = D_{t_0} \setminus B$  when  $t \in [t_0 - \delta, t_0 + \delta]$  and the deformation of  $D_t \cap B$  proceeds in a transverse direction.

Now the point is that we can isotope  $D_{t_0-\delta}$  to  $D_{t_0+\delta}$  another way through convex discs. To do so, we first eliminate all singularities in  $\text{int}(D_{t_0-\delta})$  leaving the intersection  $D_{t_0-\delta} \cap B$  untouched. This is possible because we need only to modify the disc near 0-arcs, which are far from  $B$ . They are also far from the disc boundary, so the disc may be kept ‘in between’ the discs  $D_0, D_1$ .

All singularities in the interior of the disc can be eliminated for the following reason. There are no singularities in  $\text{int}(D_0)$ , which implies that  $\mathcal{F}(D_0)$  has a single dividing curve. This is equivalent to  $\text{tb}_+(\partial D_0; D_0) = -1$ , and this number is preserved during an isotopy. So,  $\mathcal{F}(D_{t_0-\delta})$  also has a single dividing curve, hence all singularities in the interior can be eliminated.

When all singularities are eliminated from  $\text{int}(D_{t_0-\delta})$  the 1-arc is no longer present, so the desired isotopy inside  $B$  can be performed keeping the disc convex. Then the elimination of singularities is reversed, and we obtain  $D_{t_0+\delta}$ . Doing so for all passages through the 1-arc obstruction gives an isotopy from  $D_0$  to  $D_1$  through convex discs only.  $\square$

**4.6. Annuli with Legendrian boundary.** Convex annuli with Legendrian boundary and a single dividing curve are building blocks for more general convex surfaces. Any closed convex surface in  $\mathbb{S}^3$  as well as any orientable convex surface  $F$  with boundary such that  $\text{tb}_+(K; F) = 0$  for every component  $K$  of  $\partial F$  can be composed of such blocks.

Let  $A$  be such an annulus. It is bounded by two Legendrian knots that are obviously isotopic. But are they always equivalent as Legendrian knots? If the answer is positive, then a more general statement

is true: if  $A$  is an annulus with Legendrian boundary whose components have zero Thurston–Bennequin numbers relative to  $A$ , then they are equivalent as Legendrian knots.

This question was addressed in [17] and the statement was claimed to be true. However, the argument in [17] is incomplete. Up to this writing the problem appears to be open.

Theorem 2 have the following corollary for convex annuli, which may be useful to solve the above mentioned problem.

**Proposition 16.** *Let  $A$  be a convex annuli with a single dividing curve. Then it is equivalent to the convex surface  $\widehat{\Pi}$ , where  $\Pi = \{r_1, \dots, r_k = r_0\}$  is a rectangular diagram such that, for each  $i = 1, \dots, k$ , the rectangle  $r_{i-1}$  shares with  $r_i$  a single vertex that is top right for  $r_{i-1}$  and bottom left for  $r_i$ .*

*Proof.* Let  $\Pi$  be an arbitrary rectangular diagram of a surface such that  $\widehat{\Pi}$  is equivalent to  $A$ . Such a diagram exists by Theorem 2. The surface  $\widehat{\Pi}$  has a single dividing curve, which means (see the end of Subsection 4.4) that  $\Pi$  has the form  $\{r_1, \dots, r_k = r_0\}$ , where the top right vertex of  $r_{i-1}$  coincides with the bottom left vertex of  $r_i$ ,  $i = 1, \dots, k$ . If they share no more vertices we are done.

If some rectangles in  $\Pi$  share two vertices, we can find an edge  $e$  of the diagram  $\partial\Pi$  endowed with the boundary framing induced by  $\Pi$  such that some point  $v$  in  $e$  is the top left vertex of one rectangle from  $\Pi$  and the bottom right for another. Then we can ‘cut’ the diagram at the ‘wrong’ vertex and get a diagram with the same number of rectangles but longer boundary, see Fig. 34. After finitely many such

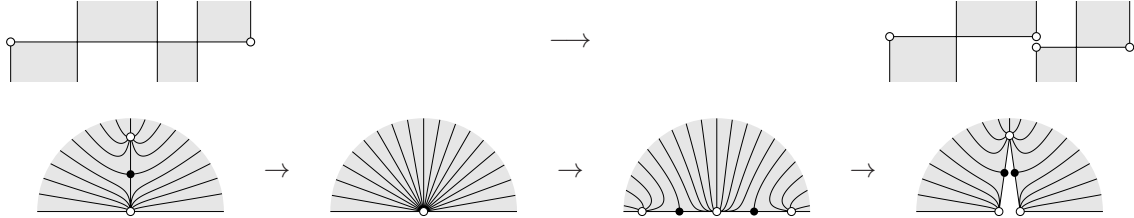


FIGURE 34. Simplifying an annulus

cuts no two rectangles will share more than one vertex.

We claim that such cuts produce an equivalent convex surface. To see this we switch from  $\widehat{\Pi}$  to  $\widehat{\Pi}^\kappa$  with  $\kappa > 0$ . For  $\widehat{\Pi}^\kappa$  the discussed operation means cutting along an edge of the Giroux graph such that exactly one endpoint of this edge lies at the boundary of the annulus. The same result can be obtained by a continuous deformation consisting of four stages: elimination of a node-saddle pair in the interior of the annulus, creation of two new node-saddle pairs at the boundary, angle adjustment, contact isotopy. This is sketched in Fig. 34.  $\square$

**Conjecture 1.** *The two boundary components of the annulus represented by the rectangular diagram in Fig. 35 are not equivalent as Legendrian knots.*

To construct the example we used a generalization of rectangular diagrams of surfaces that corresponds to branched surfaces (in the sense of [14]), which in our particular case have the form of an  $I$ -bundle over a train track. Such presentation is more compact and allows us to work with infinite series of surfaces each series presented by a single ‘branched’ diagram.

Author’s experience shows that to find simpler examples for which the equivalence of the two boundary components would not be obvious is pretty hard. It happens very often that the knots can be transformed into each other by exchange moves. The example in Fig. 35 is not such, both components of the boundary  $\partial\Pi$  are rigid in a sense that they don’t admit any exchange move. This fact may be used in the future to prove that they are not equivalent, since establishing that some kind of ‘rectangular’ surfaces does not exist for the given knot becomes much easier if the diagram is rigid. (For instance, it requires very little work to show that the knots in our example are hyperbolic.)



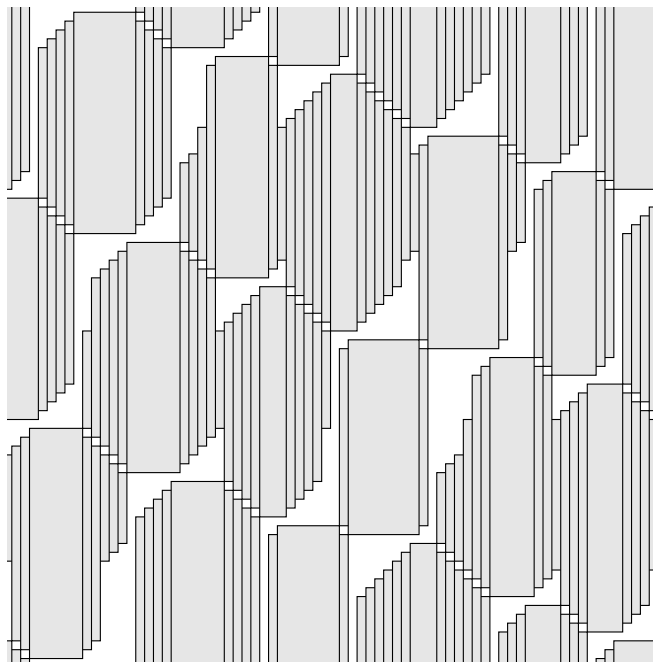


FIGURE 35. A rectangular diagram of an annulus

The known algebraic invariants do not seem to help to distinguish our knots as most of them are just too hard to compute, whereas the Pushkar–Chekanov invariant [30] is computable at some effort but vanishes for both.

## REFERENCES

- [1] D. Bennequin. Entrelacements et equations de Pfaff, *Asterisque* **107–108** (1983), 87–161.
- [2] W. Chongchitmate, L. Ng. An atlas of Legendrian knots, *Exp. Math.* **22** (2013), no. 1, 26–37.
- [3] V. Colin. Chirurgies d’indice un et isotopies de sphères dans les variétés de contact tendues, *C. R. Acad. Sci. Paris Sér. I Math.* **324** (1997), no. 6, 659–663.
- [4] V. Colin, E. Giroux, K. Honda. Finitude homotopique et isotopique des structures de contact tendues, *Publications mathématiques de l’IHÉS* **109** (2009), no. 1, 245–293.
- [5] I. Dynnikov. Arc-presentations of links: Monotonic simplification, *Fund. Math.* **190** (2006), 29–76.
- [6] I. A. Dynnikov, M. V. Prasolov. Bypasses for rectangular diagrams. A proof of the Jones conjecture and related questions (Russian), *Trudy MMO* **74** (2013), no. 1, 115–173; translation in *Trans. Moscow Math. Soc.* **74** (2013), no. 1, 97–144.
- [7] Y. Eliashberg, Contact 3-manifolds twenty years since J. Martinet’s work, *Annales de l’institut Fourier* (1992), **42**, no. 1–2, 165–192.
- [8] Y. Eliashberg, M. Fraser. Classification of topologically trivial legendrian knots, *CRM Proc. Lecture Notes*, (1998), **15**, no. 15, 17–51.
- [9] Y. Eliashberg, M. Fraser. Topologically trivial Legendrian knots, *J. Symplectic Geom.*, **7**, no. 2, (2009), 77–127.
- [10] J. Etnyre, K. Honda. On the nonexistence of tight contact structures, *Ann. of Math. (2)* **153** (2001), no. 3, 749–766.
- [11] J. Etnyre, K. Honda. Cabling and transverse simplicity, *Ann. of Math. (2)* **162** (2005), no. 3, 1305–1333.
- [12] J. Etnyre, J. Van Horn-Morris. Fibered transverse knots and the Bennequin bound, *IMRN* (2011), 1483–1509.
- [13] E. Giroux. Convexité en topologie de contact, *Comment. Math. Helv.* **66** (1991), 637–677.
- [14] W. Floyd and U. Oertel. Incompressible surfaces via branched surfaces. *Topology* **23** (1984), 117–125.
- [15] H. Geiges. *An Introduction to Contact Topology*, Cambridge University Press (2008).
- [16] E. Giroux. Structures de contact en dimension trois et bifurcations des feuilletages de surfaces, *Invent. Math.* **141** (2000), no. 3, 615–689.
- [17] G. Gospodinov. Relative Knot Invariants: Properties and Applications, *preprint* arXiv:0909.4326.
- [18] K. Honda. On the classification of tight contact structures I, *Geometry & Topology* **4** (2000), 309–368.
- [19] K. Honda. 3-dimensional methods in contact geometry, in *Different Faces of Geometry*, Edited by Donaldson et al., Kluwer Academic/Plenum Publishers, New York, 2004.
- [20] T. Ito, K. Kawamuro. Open book foliation, *Geometry & Topology* **18** (2014), 1581–1634.

- [21] Y. Kanda. The classification of tight contact structures on the 3-torus, *Comm. Anal. Geom.* **5** (1997), no. 3, 413–438.
- [22] M. Lackenby. A polynomial upper bound on Reidemeister moves, *Ann. of Math. (2)* **182** (2015), no. 2, 491–564.
- [23] C. Manolescu, P. Ozsváth, S. Sarkar. A combinatorial description of knot Floer homology, *Annals of Mathematics* (2) **169** (2009), 633–660.
- [24] P. Massot. Geodesible contact structures on 3-manifolds, *Geometry & Topology* **12** (2008) 1729–1776.
- [25] P. Massot. Topological methods in 3-dimensional Contact geometry, *preprint*, arXiv:1303.1063.
- [26] S. V. Matveev. *Algorithmic topology and classification of 3-manifolds*, Springer 2003.
- [27] D. O’Donnol, E. Pavelescu. On Legendrian Graphs, *Algebraic & Geometric Topology* (2012), **12**, no. 3, 1273–1299.
- [28] L. Ng, D. Thurston. Grid diagrams, braids, and contact geometry, *Proceedings of Gökova Geometry–Topology Conference* (2008), 120–136; Gökova Geometry–Topology Conference (GGT), Gökova, 2009.
- [29] M. Prasolov. Rectangular Diagrams of Legendrian Graphs, *Journal of Knot Theory and Its Ramifications* **23** (2014), no. 13, 1450074.
- [30] P. Pushkar’, Yu., Chekanov. Combinatorics of fronts of Legendrian links and the Arnol’d 4-conjectures (Russian), *Uspekhi Mat. Nauk* **60** (2005), no. 1, 99–154; translation in *Russian Mathematical Surveys* **60** (2005), no. 1, 95–149.

STEKLOV MATHEMATICAL INSTITUTE OF RUSSIAN ACADEMY OF SCIENCES, 8 GUBKINA STR., MOSCOW 119991, RUSSIA

*E-mail address:* dynnikov@mech.math.msu.su

*E-mail address:* 0x00002a@gmail.com